



CERN-EP-2021-208
 LHCb-PAPER-2021-038
 May 12, 2022

Tests of lepton universality using $B^0 \rightarrow K_S^0 \ell^+ \ell^-$ and $B^+ \rightarrow K^+ \ell^+ \ell^-$ decays

LHCb collaboration[†]

This paper is dedicated to the memory of our friend and colleague Sheldon Stone.

Abstract

Tests of lepton universality in $B^0 \rightarrow K_S^0 \ell^+ \ell^-$ and $B^+ \rightarrow K^+ \ell^+ \ell^-$ decays where ℓ is either an electron or a muon are presented. The differential branching fractions of $B^0 \rightarrow K_S^0 e^+ e^-$ and $B^+ \rightarrow K^+ e^+ e^-$ decays are measured in intervals of the dilepton invariant mass squared. The measurements are performed using proton-proton collision data recorded by the LHCb experiment, corresponding to an integrated luminosity of 9 fb^{-1} . The results are consistent with the Standard Model and previous tests of lepton universality in related decay modes. The first observation of $B^0 \rightarrow K_S^0 e^+ e^-$ and $B^+ \rightarrow K^+ e^+ e^-$ decays is reported.

Published in Phys. Rev. Lett. 128, 191802

© 2022 CERN for the benefit of the LHCb collaboration. CC BY 4.0 licence.

[†]Authors are listed at the end of this paper.

The $B^0 \rightarrow K_S^0 \ell^+ \ell^-$ and $B^+ \rightarrow K^{*+} \ell^+ \ell^-$ decays, where ℓ refers to either an electron or a muon, are flavour-changing neutral current (FCNC) transitions involving the transformation of a beauty quark into a strange quark.¹ These decays proceed via higher order electroweak processes in the Standard Model (SM) due to the absence of first order FCNC transitions, making them highly suppressed. Therefore, these decays may receive significant contributions from new quantum fields that lie beyond the Standard Model (BSM) and hence are promising laboratories for new physics (NP) searches.

In recent years, studies of similar $b \rightarrow s \ell^+ \ell^-$ transitions, most prominently $B^+ \rightarrow K^+ \ell^+ \ell^-$ and $B^0 \rightarrow K^{*0} \ell^+ \ell^-$ decays, have revealed tensions with the SM predictions. Deviations have been seen in ratios of branching fractions

$$R_H \equiv \frac{\int_{q_{\min}^2}^{q_{\max}^2} \frac{d\mathcal{B}(B \rightarrow H \mu^+ \mu^-)}{dq^2} dq^2}{\int_{q_{\min}^2}^{q_{\max}^2} \frac{d\mathcal{B}(B \rightarrow H e^+ e^-)}{dq^2} dq^2}, \quad (1)$$

where B denotes a B^+ or a B^0 meson, H is either a K or a K^* meson, and q^2 is the dilepton invariant mass squared. In the SM the charged leptons have identical interaction strengths, which is referred to as lepton universality. The only exception is their interaction with the Higgs field, which determines their differing masses. Therefore, these ratios are predicted to be very close to unity [1], with corrections from QED up to $\mathcal{O}(10^{-2})$ [2, 3] and further small corrections due to the muon-electron mass difference. Furthermore, these ratios benefit from precise cancellation of the hadronic uncertainties that affect predictions of the branching fractions and angular observables, which affect the ratios at $\mathcal{O}(10^{-4})$ [4]. Significant deviation from unity in such ratios would therefore constitute unambiguous evidence of BSM physics.

The ratio $R_{K^{*0}}$, measured by the LHCb collaboration using the data collected in the q^2 regions $0.045 < q^2 < 1.1 \text{ GeV}^2/c^4$ and $1.1 < q^2 < 6.0 \text{ GeV}^2/c^4$ [5], is in tension with the SM predictions at 2.2–2.4 and 2.4–2.5 standard deviations (σ), respectively, where the ranges are due to the use of different Standard Model predictions. A measurement of R_{K^+} performed in the region $1.1 < q^2 < 6.0 \text{ GeV}^2/c^4$ deviates from the SM by 3.1 standard deviations [6]. The analogous ratio measured using $\Lambda_b^0 \rightarrow p K^- \ell^+ \ell^-$ decays, R_{pK} , is consistent with the SM within one standard deviation [7]. All four measurements show a deficit of $b \rightarrow s \mu^+ \mu^-$ decays with respect to $b \rightarrow s e^+ e^-$ decays.

In addition, angular observables [8–19] and branching fractions [20–23] of $b \rightarrow s \mu^+ \mu^-$ decays have been measured, with several in tension with the SM. However, the extent to which they may be affected by residual quantum chromodynamics contributions remains uncertain [24–34].

Intriguingly, it is possible to account for all these anomalies simultaneously through the modification of the $b \rightarrow s$ coupling in a model-independent way [35–46]. Such a modification can be generated by the presence of a heavy neutral boson [47–63] or a leptoquark [64–90], as well as in models with supersymmetry [91–93], extra dimensions [94], and extended Higgs sectors [95–99].

The $B^0 \rightarrow K_S^0 \ell^+ \ell^-$ and $B^+ \rightarrow K^{*+} \ell^+ \ell^-$ decays are the isospin partners of $B^+ \rightarrow K^+ \ell^+ \ell^-$ and $B^0 \rightarrow K^{*0} \ell^+ \ell^-$ decays and are expected to be affected by the same

¹Charge conjugate processes are implied throughout.

NP contributions. Testing lepton universality by measuring the ratios $R_{K_S^0}$ and $R_{K^{*+}}$ can therefore provide important additional evidence for or against NP. However, while these decays have similar branching fractions to their isospin partners, $\mathcal{O}(10^{-6})$ to $\mathcal{O}(10^{-7})$, they suffer from a reduced experimental efficiency at LHCb due to the presence of a long-lived K_S^0 meson in the final state. These ratios have previously been measured by the BaBar [100] and Belle [101, 102] collaborations. The differential branching fractions of the muon modes, $B^0 \rightarrow K_S^0 \mu^+ \mu^-$ and $B^+ \rightarrow K^{*+} \mu^+ \mu^-$, were found to be lower although still consistent with predictions at low q^2 in a measurement performed by the LHCb collaboration [22]. No single experiment has unambiguously observed the electron decay modes to date.

In this Letter, measurements of the ratios $R_{K_S^0}$ and $R_{K^{*+}}$ and the differential branching fractions of $B^0 \rightarrow K_S^0 e^+ e^-$ and $B^+ \rightarrow K^{*+} e^+ e^-$ decays are presented. The measurements are performed using proton-proton (pp) collision data corresponding to an integrated luminosity of 9 fb^{-1} recorded by the LHCb experiment in 2011, 2012 (Run 1) and 2016–2018 (Run 2) at centre-of-mass energies of 7, 8 and 13 TeV, respectively. The K_S^0 and K^{*+} mesons are reconstructed in the $\pi^+ \pi^-$ and $K_S^0 \pi^+$ final states, respectively. The ratio $R_{K_S^0}$ and the branching fraction $\mathcal{B}(B^0 \rightarrow K_S^0 e^+ e^-)$ are measured in the region $1.1 < q^2 < 6.0 \text{ GeV}^2/c^4$, while $R_{K^{*+}}$ and $\mathcal{B}(B^+ \rightarrow K^{*+} e^+ e^-)$ are determined in the range $0.045 < q^2 < 6.0 \text{ GeV}^2/c^4$. A wider range is used in the case of the B^+ decay, the differential branching fraction of which is enhanced at low q^2 by the photon pole, since the K^{*+} is a vector meson. Splitting the q^2 range into two bins at $1.1 \text{ GeV}^2/c^4$, as was done in the $R_{K^{*0}}$ measurement, is not possible due to the limited data sample.

The analysis is designed to minimise systematic uncertainties, particularly those associated with differences in the detector response between electrons and muons. The ratios and differential branching fractions are normalised to the control modes, $B^0 \rightarrow J/\psi(e^+ e^-) K_S^0$, $B^0 \rightarrow J/\psi(\mu^+ \mu^-) K_S^0$, $B^+ \rightarrow J/\psi(e^+ e^-) K^{*+}$, and $B^+ \rightarrow J/\psi(\mu^+ \mu^-) K^{*+}$, the branching fractions of which are known to respect lepton universality to an excellent approximation [103] and are taken to be equal for the muon and the electron decays of a given B meson. The parameters $R_{K_S^0}^{-1}$ and $R_{K^{*+}}^{-1}$ are measured as double ratios

$$\begin{aligned} R_{K^{(*)}}^{-1} &= \frac{\mathcal{B}(B \rightarrow K^{(*)} e^+ e^-)}{\mathcal{B}(B \rightarrow J/\psi(e^+ e^-) K^{(*)})} / \frac{\mathcal{B}(B \rightarrow K^{(*)} \mu^+ \mu^-)}{\mathcal{B}(B \rightarrow J/\psi(\mu^+ \mu^-) K^{(*)})} \\ &= \left(\frac{N_{\text{sig}}^{ee}}{\epsilon_{\text{sig}}^{ee}} \cdot \frac{\epsilon_{\text{con}}^{ee}}{N_{\text{con}}^{ee}} \right) / \left(\frac{N_{\text{sig}}^{\mu\mu}}{\epsilon_{\text{sig}}^{\mu\mu}} \cdot \frac{\epsilon_{\text{con}}^{\mu\mu}}{N_{\text{con}}^{\mu\mu}} \right), \end{aligned} \quad (2)$$

where $K^{(*)}$ is either a K_S^0 or K^{*+} meson, N is the measured yield, and ϵ is the total efficiency for signal (sig) and control (con) decays. The inverse ratio $R_{K^{(*)}}^{-1}$ is measured as its uncertainty better represents a Gaussian distribution due to the low yield of the electron decay mode. Many sources of systematic bias cancel in the ratio between the signal and control modes. The differential branching fractions of the signal electron modes are measured as

$$\frac{d\mathcal{B}(B \rightarrow K^{(*)} e^+ e^-)}{dq^2} = \frac{N_{\text{sig}}^{ee}}{\epsilon_{\text{sig}}^{ee}} \frac{\epsilon_{\text{con}}^{ee}}{N_{\text{con}}^{ee}} \frac{\mathcal{B}(B \rightarrow J/\psi(e^+ e^-) K^{(*)})}{q_{\text{max}}^2 - q_{\text{min}}^2}. \quad (3)$$

The LHCb detector is a single-arm forward spectrometer covering the pseudorapidity range $2 < \eta < 5$, described in detail in Refs. [104, 105]. The simulated events used in

this analysis are produced with the software described in Refs. [106–110]. In particular, final-state radiation is simulated using PHOTOS [111].

The candidates used in the analysis must first pass a hardware trigger, which requires the presence of at least one muon with high transverse momentum, p_T , in the case of $B \rightarrow K^{(*)}\mu^+\mu^-$ candidates, or in the case of $B \rightarrow K^{(*)}e^+e^-$ candidates at least one electron or hadron with large energy deposits in the electromagnetic calorimeter (ECAL) or hadronic calorimeter (HCAL), respectively. Further $B \rightarrow K^{(*)}e^+e^-$ candidates are selected where the hardware trigger requirements are satisfied by objects from the underlying pp collision that do not form part of the reconstructed candidate. Candidates are then required to pass a software trigger, the first stage of which requires the presence of at least one track with high p_T that is well separated from the primary pp interaction vertex (PV), followed by a second stage that imposes topological requirements on the final-state tracks to determine whether they are consistent with the decay of a b hadron.

Muons are initially identified from tracks that penetrate the calorimeters and the iron absorber plates of the muon system and further separated from hadrons (primarily pions and kaons) by a multivariate classifier that combines information from the other subdetectors. Electrons are identified from tracks with an associated deposit of energy in the ECAL, and separated from hadrons using a similar multivariate classifier.

Due to their small mass, electrons lose energy via bremsstrahlung radiation as they traverse the detector material, leading to a degradation in their energy and momentum resolution. A bremsstrahlung recovery procedure is used to identify energy deposits in the ECAL that are consistent with photons radiated from electron candidate tracks upstream of the magnet. This is done by extrapolating the direction of the electron track before the magnet to a position in the ECAL and then searching for energy deposits without associated tracks at that location. When such a deposit is identified, its energy is used to correct the electron’s energy and momentum. This leads to an improvement in the B candidate invariant mass resolution, although the resolution for electronic modes remains larger than for the equivalent muonic channels.

Candidate K_S^0 mesons are reconstructed from two oppositely charged tracks identified as pions, using either a pair of tracks that originate in the vertex locator (long tracks), or two tracks that originate downstream of the vertex locator in the first silicon-strip detector (downstream tracks). Around a third of reconstructed K_S^0 mesons are formed from long tracks. Candidate $B^0 \rightarrow K_S^0\ell^+\ell^-$ decays are formed from two oppositely charged tracks identified as either muons or electrons combined with a candidate K_S^0 meson. In the case of $B^+ \rightarrow K^{*+}\ell^+\ell^-$ candidates, the additional charged pion is required to result in a $K_S^0\pi^+$ mass within $300\text{ MeV}/c^2$ of the K^{*+} mass [103]. An estimated S-wave contribution in this K^{*+} mass window of approximately 22% based on previous studies of $B^0 \rightarrow K^+\pi^-\mu^+\mu^-$ decays by the LHCb collaboration [20] is included in the analysis. When measuring the $B^+ \rightarrow K^{*+}e^+e^-$ differential branching fraction, the $B^+ \rightarrow J/\psi(e^+e^-)K^{*+}$ control mode is selected with a $K_S^0\pi^+$ mass in the range $792 - 992\text{ MeV}/c^2$ in order to be consistent with the selection used in previous measurements of $\mathcal{B}(B^+ \rightarrow J/\psi K^{*+})$ [112, 113], the world average of which is taken as external input [103]. Background is further suppressed by requirements on the quality of the B decay vertex, the flight distance significance of the B candidate, how consistent the B candidate is with having originated at the PV, the invariant masses of the K_S^0 , K^{*+} and B candidates, and the p_T and separation from the PV of the final-state tracks. In an additional step, the invariant masses of B candidates are recalculated with the K_S^0 meson mass constrained to its measured value [103], leading

to an improvement in the B mass resolution.

Various requirements on decay kinematics, decay time, and particle identification (PID) information are used to reject potential background originating from misidentified b -hadron (H_b) decays. Background to $B^0 \rightarrow K_S^0 \ell^+ \ell^-$ decays includes $H_b \rightarrow hh' \ell^+ \ell^-$ decays (where h refers to a hadron), $\Lambda_b^0 \rightarrow \Lambda \ell^+ \ell^-$ and $B^0 \rightarrow D^- (K_S^0 X) Y$ decays, where both X and Y represent either an electron-neutrino pair or a pion. Background to $B^+ \rightarrow K^{*+} \ell^+ \ell^-$ decays includes $B^0 \rightarrow K_S^0 \ell^+ \ell^-$ decays combined with a random additional pion, $B^+ \rightarrow J/\psi(\ell^+ \ell^-) K^{*+}$ and $B^+ \rightarrow \psi(2S)(\ell^+ \ell^-) K^{*+}$ decays where the companion pion from the K^{*+} is swapped with a lepton from the J/ψ or $\psi(2S)$ meson, $H_b \rightarrow hh' \pi \ell^+ \ell^-$ decays, decays with Λ baryons in the final state, and $B^+ \rightarrow \bar{D}^0 (K_S^0 \pi^+ X) Y$ decays. These selection requirements reduce all these background sources to levels that have a negligible (sub-percent) effect on the measured signal yields. The $B^0 \rightarrow K_S^0 \pi^+ \pi^-$ and $B^+ \rightarrow K^{*+} \pi^+ \pi^-$ decays, where the pions are misidentified as electrons, are significantly reduced by the electron particle identification requirements and included as components in the mass fits.

Multivariate classifiers based on boosted decision tree (BDT) algorithms [114] are used to suppress background from coincidental track combinations (combinatorial background). Separate classifiers are trained for each signal decay mode, the two data-taking periods (Run 1, Run 2) and whether the K_S^0 meson was reconstructed from long or downstream tracks. Each classifier is trained on a signal sample of simulated $B \rightarrow K^{(*)} \ell^+ \ell^-$ decays, and a background sample taken from data with a reconstructed invariant B mass greater than $5500 \text{ MeV}/c^2$ and q^2 regions consistent with either a J/ψ or $\psi(2S)$ meson removed. The classifiers combine information on the B candidate's fit quality, distance of closest approach to the PV, flight distance, p_T and decay time; the decay time of the dilepton pair; the p_T and decay time of the K_S^0 candidate; how isolated the B , dilepton and K_S^0 candidates are from other tracks in the event; and the distance of closest approach to the PV of long tracks forming the K_S^0 candidate. Requirements on the classifier outputs are optimised to provide the maximum signal significance, defined as $S/\sqrt{S+B}$, where S is the expected signal calculated from the control mode yield in data, the signal-to-control mode efficiency ratio from simulation and the signal-to-control mode branching fraction ratio [103], and B is the background yield in the signal region, extrapolated from a fit to the data mass sidebands.

The muon and electron control modes are selected in the ranges of $8.98 < q^2 < 10.21 \text{ GeV}^2/c^4$ and $6.0 < q^2 < 11.0 \text{ GeV}^2/c^4$, respectively, and the spectra of their invariant masses $m(J/\psi K_S^0)$ and $m(J/\psi K_S^0 \pi^+)$ are shown in Fig. 1. Their yields are determined using fits to the B candidate mass, calculated with the masses of the K_S^0 and J/ψ mesons constrained to their measured values [103], improving the resolution. The mass distribution of each control mode is modelled with a sum of two Crystal Ball functions [115] with common mean and opposite-side power law tails (referred to as a double Crystal Ball or DCB), with parameters fixed to values obtained from fits to simulated events. The muon control modes are modelled using a single DCB function, while the electron control modes are modelled using a sum of three DCB functions, where the shape of each component and their relative fractions are determined from fits to simulation in three different categories according to the number of bremsstrahlung photons added to the candidate's electrons: 0, 1, or ≥ 2 . In the fit to data, shifts in the DCB means and widths are allowed to vary freely with respect to those obtained from simulation in order to accommodate data-simulation differences in the mass scale

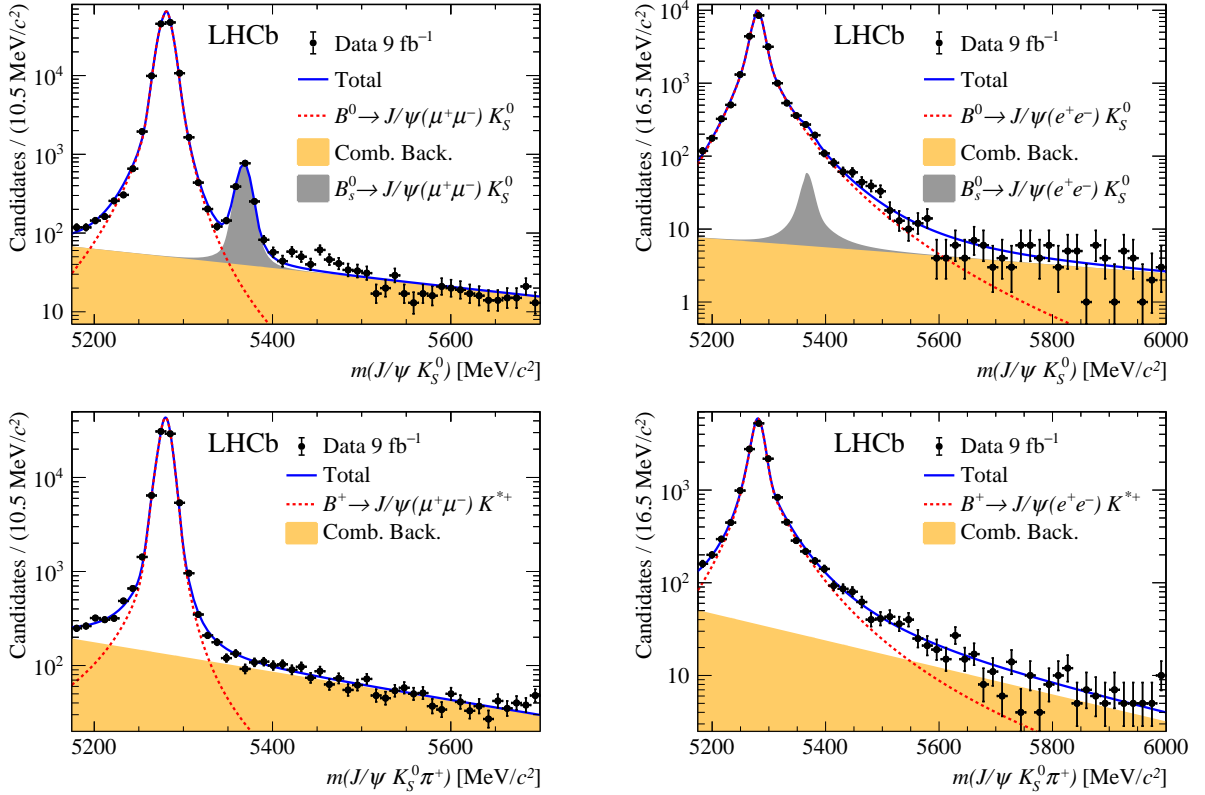


Figure 1: Distributions of (top left) $J/\psi(\mu^+\mu^-)K_S^0$ mass, (top right) $J/\psi(e^+e^-)K_S^0$ mass, (bottom left) $J/\psi(\mu^+\mu^-)K_S^0\pi^+$ mass and (bottom right) $J/\psi(e^+e^-)K_S^0\pi^+$ mass with the fit models used to determine the control mode yields.

and resolution. Combinatorial background is modelled with an exponential function. In the case of the B^0 control modes, $B_s^0 \rightarrow J/\psi(\ell^+\ell^-)K_S^0$ decays are modelled with the B^0 DCB function with its mean offset by the measured $m_{B_s^0} - m_{B^0}$ mass difference [103] and with its yield allowed to vary freely. The lower limit of the mass range excludes partially reconstructed background from higher K^* resonances, which are not modelled. The structures visible in the range $5400 \text{ MeV}/c^2 < m(J/\psi K_S^0) < 5500 \text{ MeV}/c^2$ are due to small amounts of residual contamination from Λ_b^0 decays, which have a negligible effect on the measured yields of $B^0 \rightarrow J/\psi(\mu^+\mu^-)K_S^0$ and $B^0 \rightarrow J/\psi(e^+e^-)K_S^0$ decays. The results of the fit are shown in Fig. 1 and the yields of $B^0 \rightarrow J/\psi(\mu^+\mu^-)K_S^0$, $B^0 \rightarrow J/\psi(e^+e^-)K_S^0$, $B^+ \rightarrow J/\psi(\mu^+\mu^-)K^{*+}$, and $B^+ \rightarrow J/\psi(e^+e^-)K^{*+}$ decays are found to be $118\,750 \pm 360$, $21\,080 \pm 170$, $75\,420 \pm 290$, and $14\,330 \pm 170$, respectively.

The spectra of the invariant masses $m(K_S^0\mu^+\mu^-)$, $m(K_S^0e^+e^-)$, $m(K_S^0\pi^+\mu^+\mu^-)$, and $m(K_S^0\pi^+e^+e^-)$ of the muon and electron signal modes are shown in Fig. 2. The yields of $B^0 \rightarrow K_S^0\mu^+\mu^-$ and $B^+ \rightarrow K^{*+}\mu^+\mu^-$ decays are determined using fits to the $K_S^0\mu^+\mu^-$ and $K_S^0\pi^+\mu^+\mu^-$ mass distributions. The $B^0 \rightarrow K_S^0\mu^+\mu^-$ and $B^+ \rightarrow K^{*+}\mu^+\mu^-$ signal decays are modelled using DCB functions where the shape parameters are determined from fits to simulation, with shifts in their means and widths taken from the corresponding control mode fits to data. Combinatorial background is modelled using an exponential function, while partially reconstructed background is excluded by the lower mass limit.

The ratios and branching fractions are determined using fits to $K_S^0e^+e^-$ and $K_S^0\pi^+e^+e^-$

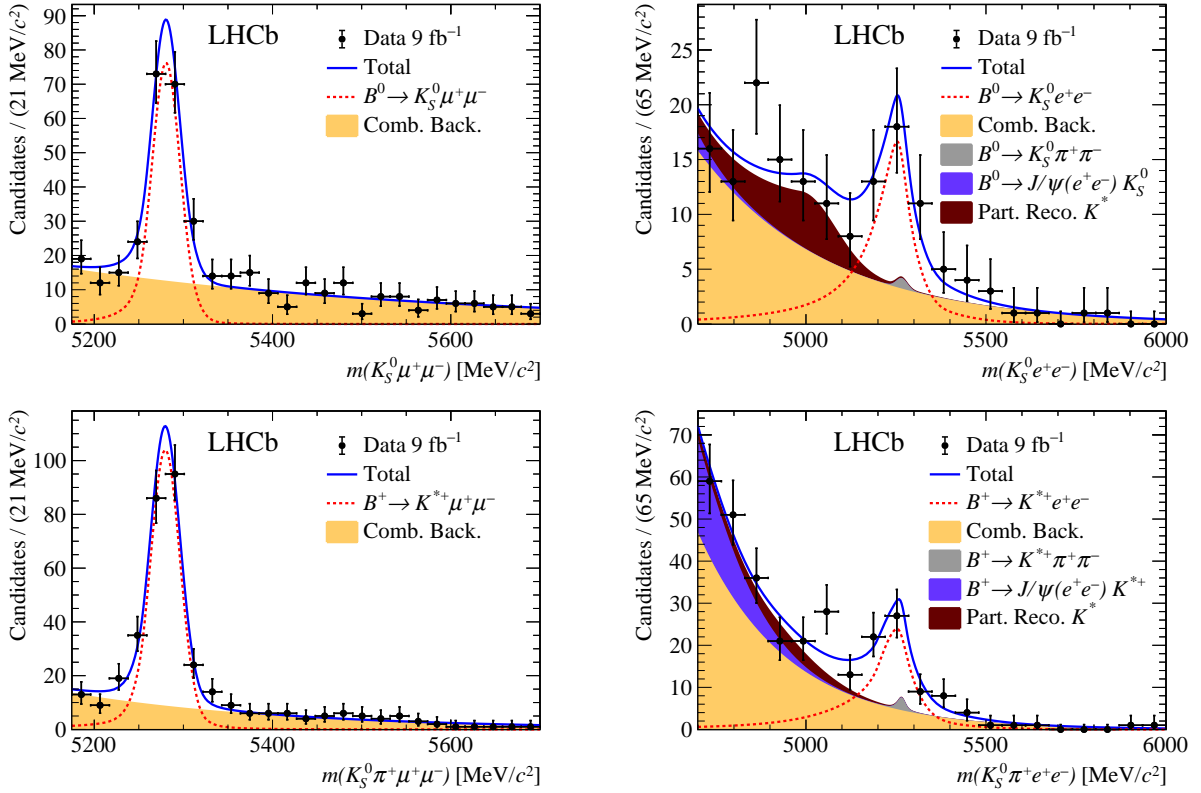


Figure 2: Distributions of (top left) $K_S^0\mu^+\mu^-$ and (top right) $K_S^0e^+e^-$ mass with the fit models used to determine the $B^0 \rightarrow K_S^0\mu^+\mu^-$ yield and $R_{K_S^0}^{-1}$, and (bottom left) $K_S^0\pi^+\mu^+\mu^-$ and (bottom right) $K_S^0\pi^+e^+e^-$ mass with the fit models used to determine the $B^+ \rightarrow K^{*+}\mu^+\mu^-$ yield and $R_{K^{*+}}^{-1}$.

mass spectra, with the K_S^0 candidate's mass constrained to its measured value. The $B^0 \rightarrow K_S^0e^+e^-$ and $B^+ \rightarrow K^{*+}e^+e^-$ signal decays are modelled using the sum of three DCB functions, each corresponding to different numbers of recovered bremsstrahlung photons. The DCB parameters are taken from simulation with shifts in the means and widths taken from the control mode fits to data without a J/ψ mass constraint. Partially reconstructed background from higher K^* resonances is modelled using a DCB function with shape parameters constrained from simulation in the $B^0 \rightarrow K_S^0e^+e^-$ fit, and Gaussian kernel density estimations (KDE) determined from simulation in the $B^+ \rightarrow K^{*+}e^+e^-$ fit, with their yields allowed to vary freely. Leakage from the J/ψ control modes into the signal region is modelled using KDE functions, with their yields constrained based on the control mode fits and the efficiency in simulation. Residual contamination from $B^0 \rightarrow K_S^0\pi^+\pi^-$ and $B^+ \rightarrow K^{*+}\pi^+\pi^-$ decays is modelled in each fit by a DCB function determined from simulated events, with its yield constrained using the control mode yields, the control mode and background branching fractions, and the efficiencies taken from simulation. Combinatorial background is modelled with an exponential function.

The efficiencies used in the measurements of the ratios and differential branching fractions are calculated using simulation, to which various corrections are applied to improve the agreement with data. The PID efficiencies for each channel are calculated from calibration data samples of electrons, muons and pions, and are applied as per-

candidate weights to the simulation. Similarly, the electron tracking efficiency is corrected using calibration samples. The p_T and pseudorapidity of the B mesons generated by PYTHIA 8 [106], and the occupancy of the underlying events are corrected by comparing their distributions between data and simulation using the muon control modes to calculate per-candidate weights, which are applied to both electron and muon samples. Similarly, the trigger efficiency is corrected by comparing the efficiency as a function of the p_T of the muons, the transverse energy of the electrons and pions, and the p_T of the B meson, between control mode data and simulation. Further weights are applied to correct any residual mismodelling of the BDT classifier response. Finally, the simulated q^2 distribution is corrected using control mode data to account for the larger observed resolution in data.

Multiple sources of systematic uncertainty are evaluated, the largest of which comes from the statistical uncertainties of the efficiencies due to the sizes of the available samples of simulated events. These affect the $R_{K^{(*)}}^{-1}$ ratios and the differential branching fractions at 2–3%. The next largest are associated with the mass fit models, in particular the limited size of the simulation samples used to determine the shape parameters, and the choices of models used for the partially reconstructed and J/ψ leakage background, which affect the observables by 1–2%. The remaining sources of systematic uncertainty are found to be close to or below the 1% level. These include: the limited amount of data and simulation used to calculate correction weights; the choices of binning schemes used to evaluate the PID efficiency weights and potential biases in this procedure due to correlations in the PID response between the two electrons; the choice of methods used to calculate the trigger efficiency; imperfect modelling of the muon track reconstruction efficiency; residual mismodelling of the BDT classifier response in simulation; residual bias in the fitting procedure evaluated using pseudoexperiments, and residual contamination from $B^0 \rightarrow D^-(K_S^0 X)Y$ and $B^+ \rightarrow \bar{D}^0(K_S^0 \pi^+ X)Y$ decays. Other sources of residual background contamination were found to have a negligible effect on the measurements. All systematic uncertainties, as well as the statistical precision of the efficiencies and various parameters used in the maximum likelihood fits, are included as Gaussian constraints in the fit. Finally, the statistical precision on each observable is scaled by factors determined from pseudoexperiments (with values in the range 1.01–1.02), in order to guarantee proper coverage.

A number of checks are performed to ensure that efficiencies are accurately estimated. The ratios $R_{\psi(2S)K^{(*)}}^{-1}$, where the signal modes in Eq. (2) are substituted for $B \rightarrow \psi(2S)(\mu^+\mu^-)K^{(*)}$ and $B \rightarrow \psi(2S)(e^+e^-)K^{(*)}$ decays, selected in the q^2 ranges $[12.86, 14.33]\text{ GeV}^2/c^4$ and $[11.0, 15.0]\text{ GeV}^2/c^4$, respectively, are found to be $R_{\psi(2S)K_S^0}^{-1} = 1.014 \pm 0.030\text{ (stat.)} \pm 0.020\text{ (syst.)}$ and $R_{\psi(2S)K^{*+}}^{-1} = 1.017 \pm 0.045\text{ (stat.)} \pm 0.023\text{ (syst.)}$, consistent with unity as expected due to lepton universality in J/ψ and $\psi(2S)$ decays [6]. Additionally, the single ratios

$$r_{J/\psi K^{(*)}}^{-1} \equiv \frac{\mathcal{B}(B \rightarrow J/\psi(e^+e^-)K^{(*)})}{\mathcal{B}(B \rightarrow J/\psi(\mu^+\mu^-)K^{(*)})} = \frac{N_{\text{con}}^{ee} \epsilon_{\text{con}}^{\mu\mu}}{N_{\text{con}}^{\mu\mu} \epsilon_{\text{con}}^{ee}}, \quad (4)$$

which do not benefit from cancellation of systematic biases between signal and control modes, and are therefore a stringent check of the efficiencies, are found to be $r_{J/\psi K_S^0}^{-1} = 0.977 \pm 0.008\text{ (stat.)} \pm 0.027\text{ (syst.)}$ and $r_{J/\psi K^{*+}}^{-1} = 0.965 \pm 0.011\text{ (stat.)} \pm 0.032\text{ (syst.)}$, again consistent with unity in both cases. Furthermore, differential measurements of $r_{J/\psi K^{(*)}}$ as functions of a range of

variables that are differently distributed in the signal and control decays are performed. The most powerful of these tests measures $r_{J/\psi K^{(*)}}$ as a function of the response of a BDT classifier trained on simulated candidates to distinguish signal and control decays. All these differential distributions are found to be flat within the statistical precision, providing further confidence that the yields and efficiencies are well estimated [116].

In order to avoid experimenter's bias, the results of the analysis and the electron signal mode mass spectra were not examined until the full procedure had been finalised and checks had been performed to ensure that the muon signal mode branching fractions were in agreement between the different data-taking years and also with the results of the previous measurements made by LHCb [22]. The fits to the $B^0 \rightarrow K_S^0 e^+ e^-$, $B^0 \rightarrow K_S^0 \mu^+ \mu^-$, $B^+ \rightarrow K^{*+} e^+ e^-$ and $B^+ \rightarrow K^{*+} \mu^+ \mu^-$ invariant-mass spectra are shown in Fig. 2. The fitted yields of $B^0 \rightarrow K_S^0 e^+ e^-$, $B^0 \rightarrow K_S^0 \mu^+ \mu^-$, $B^+ \rightarrow K^{*+} e^+ e^-$ and $B^+ \rightarrow K^{*+} \mu^+ \mu^-$ decays are 45 ± 10 , 155 ± 15 , 67 ± 13 and 221 ± 17 , respectively. The ratios $R_{K_S^0}^{-1}$ and $R_{K^{*+}}^{-1}$ are measured to be

$$R_{K_S^0}^{-1} = 1.51^{+0.40}_{-0.35} \text{ (stat.)}^{+0.09}_{-0.04} \text{ (syst.)},$$

$$R_{K^{*+}}^{-1} = 1.44^{+0.32}_{-0.29} \text{ (stat.)}^{+0.09}_{-0.06} \text{ (syst.)},$$

in the q^2 ranges $[1.1, 6.0]$ GeV^2/c^4 and $[0.045, 6.0]$ GeV^2/c^4 , respectively. These ratios are consistent with the SM at 1.5 and 1.4 standard deviations, respectively, evaluated using Wilks' theorem [117]. To aid comparison with other lepton-universality ratios, $R_{K_S^0}$ and $R_{K^{*+}}$ are calculated by inverting the results above, yielding

$$R_{K_S^0} = 0.66^{+0.20}_{-0.14} \text{ (stat.)}^{+0.02}_{-0.04} \text{ (syst.)},$$

$$R_{K^{*+}} = 0.70^{+0.18}_{-0.13} \text{ (stat.)}^{+0.03}_{-0.04} \text{ (syst.)}.$$

The differential branching fractions of the signal electron decays are found to be

$$\frac{d\mathcal{B}(B^0 \rightarrow K^0 e^+ e^-)}{dq^2} = (2.6 \pm 0.6 \text{ (stat.)} \pm 0.1 \text{ (syst.)}) \times 10^{-8} \text{ GeV}^{-2} c^4,$$

$$\frac{d\mathcal{B}(B^+ \rightarrow K^{*+} e^+ e^-)}{dq^2} = (9.2^{+1.9}_{-1.8} \text{ (stat.)}^{+0.8}_{-0.6} \text{ (syst.)}) \times 10^{-8} \text{ GeV}^{-2} c^4,$$

in the q^2 ranges $[1.1, 6.0]$ GeV^2/c^4 and $[0.045, 6.0]$ GeV^2/c^4 and where the significances of the $B^0 \rightarrow K_S^0 e^+ e^-$ and $B^+ \rightarrow K^{*+} e^+ e^-$ decays evaluated using Wilks' theorem [117] are 5.3σ and 6.0σ , respectively. Since the control mode branching fraction of $B^0 \rightarrow J/\psi K^0$ decays $(8.91 \pm 0.21) \times 10^{-4}$ [103] is used, the differential branching fraction of $B^0 \rightarrow K^0 e^+ e^-$ instead of $B^0 \rightarrow K_S^0 e^+ e^-$ decays is reported. A combination of the $R_{K_S^0}^{-1}$ and $R_{K^{*+}}^{-1}$ measurements is performed using the FLAVIO software package [118] to fit for a single muon-specific Wilson coefficient $C_9^{\text{NP}} = -C_{10}^{\text{NP}}$, while fixing all other Wilson coefficients to their SM values. This scenario is used in several existing fits to $b \rightarrow s l^+ l^-$ -data, and is chosen specifically as the ratios $R_{K^{(*)}}$ have poor sensitivity in discriminating between the Wilson Coefficients C_9 and C_{10} . The fit results in $C_9^{\text{NP}} = -C_{10}^{\text{NP}} = -0.8^{+0.4}_{-0.3}$ and a significance of 2.0 standard deviations with respect to the SM under this specific scenario. It should be noted that this fit is model-dependent and the result could change if data-driven estimates of the hadronic uncertainties were used.

These measurements constitute the most precise tests of lepton universality in $B^0 \rightarrow K_S^0 \ell^+ \ell^-$ and $B^+ \rightarrow K^{*+} \ell^+ \ell^-$ decays to date, the most precise measurements of

their differential branching fractions at low q^2 , and the first observations of $B^0 \rightarrow K_S^0 e^+ e^-$ and $B^+ \rightarrow K^*+ e^+ e^-$ decays. While these measurements are individually consistent with the SM, the central values exhibit the same deficit of muonic decays relative to electronic decays as seen in the other lepton universality tests performed by the LHCb collaboration [5–7].

Acknowledgements

We express our gratitude to our colleagues in the CERN accelerator departments for the excellent performance of the LHC. We thank the technical and administrative staff at the LHCb institutes. We acknowledge support from CERN and from the national agencies: CAPES, CNPq, FAPERJ and FINEP (Brazil); MOST and NSFC (China); CNRS/IN2P3 (France); BMBF, DFG and MPG (Germany); INFN (Italy); NWO (Netherlands); MNiSW and NCN (Poland); MEN/IFA (Romania); MSHE (Russia); MICINN (Spain); SNSF and SER (Switzerland); NASU (Ukraine); STFC (United Kingdom); DOE NP and NSF (USA). We acknowledge the computing resources that are provided by CERN, IN2P3 (France), KIT and DESY (Germany), INFN (Italy), SURF (Netherlands), PIC (Spain), GridPP (United Kingdom), RRCKI and Yandex LLC (Russia), CSCS (Switzerland), IFIN-HH (Romania), CBPF (Brazil), PL-GRID (Poland) and NERSC (USA). We are indebted to the communities behind the multiple open-source software packages on which we depend. Individual groups or members have received support from ARC and ARDC (Australia); AvH Foundation (Germany); EPLANET, Marie Skłodowska-Curie Actions and ERC (European Union); A*MIDEX, ANR, IPhU and Labex P2IO, and Région Auvergne-Rhône-Alpes (France); Key Research Program of Frontier Sciences of CAS, CAS PIFI, CAS CCEPP, Fundamental Research Funds for the Central Universities, and Sci. & Tech. Program of Guangzhou (China); RFBR, RSF and Yandex LLC (Russia); GVA, XuntaGal and GENCAT (Spain); the Leverhulme Trust, the Royal Society and UKRI (United Kingdom).

A Supplemental material

This appendix contains supplemental material to the measurements. Eq. 5 gives the the $B^0 \rightarrow K_S^0 e^+ e^-$ and $B^+ \rightarrow K^{*+} e^+ e^-$ differential branching fractions divided by the branching fractions of their respective normalisation modes. Fig. 3 shows the total efficiencies for the four signal decay modes as function of q^2 . Figs. 4 and 5 show differential measurements of $r_{J/\psi K^{(*)}}^{-1}$. Figs. 6 and 7 show the profile likelihood scans for $R_{K^{(*)}}^{-1}$ and the differential branching fractions. Fig. 8 compares the measurements of $R_{K^{(*)}}^{-1}$ presented in this Letter with previous measurements by the Belle collaboration. Fig. 9 shows the $J/\psi K^{(*)}$ invariant mass spectra and the maximum likelihood fits use to determine the $B \rightarrow J/\psi K^{(*)}$ control mode yields with a linear scale. Figs. 10 and 11 show the $\psi(2S) K^{(*)}$ invariant mass spectra and the maximum likelihood fits use to determine the $B \rightarrow \psi(2S) K^{(*)}$ mode yields with linear and logarithmic scales.

In the main text, the differential branching fractions of $B^0 \rightarrow K_S^0 e^+ e^-$ and $B^+ \rightarrow K^{*+} e^+ e^-$ decays are reported. These are normalised using the world-average branching fractions for $B^0 \rightarrow J/\psi(e^+ e^-) K^0$ and $B^+ \rightarrow J/\psi(e^+ e^-) K^{*+}$ respectively [103]. The ratios of signal and control mode branching fractions used in this calculation are

$$\begin{aligned} \frac{d\mathcal{B}(B^0 \rightarrow K^0 e^+ e^-)}{dq^2} / \mathcal{B}(B^0 \rightarrow J/\psi(e^+ e^-) K^0) &= \\ (4.9_{-1.1}^{+1.2} \text{ (stat.)} \pm 0.2 \text{ (syst.)}) \times 10^{-4} \text{ GeV}^{-2} c^4, \\ \frac{d\mathcal{B}(B^+ \rightarrow K^{*+} e^+ e^-)}{dq^2} / \mathcal{B}(B^+ \rightarrow J/\psi(e^+ e^-) K^{*+}) &= \\ (1.08_{-0.21}^{+0.22} \text{ (stat.)} \pm 0.06 \text{ (syst.)}) \times 10^{-3} \text{ GeV}^{-2} c^4, \end{aligned} \quad (5)$$

where $B^+ \rightarrow K^{*+} e^+ e^-$ candidates are selected with $m(K_S^0 \pi^+)/\text{MeV}/c^2$ within 300 MeV/ c^2 of the world-average K^{*+} mass, whereas $B^+ \rightarrow J/\psi(e^+ e^-) K^{*+}$ candidates are selected in the range $792 < m(K_S^0 \pi^+)/\text{MeV}/c^2 < 992$.

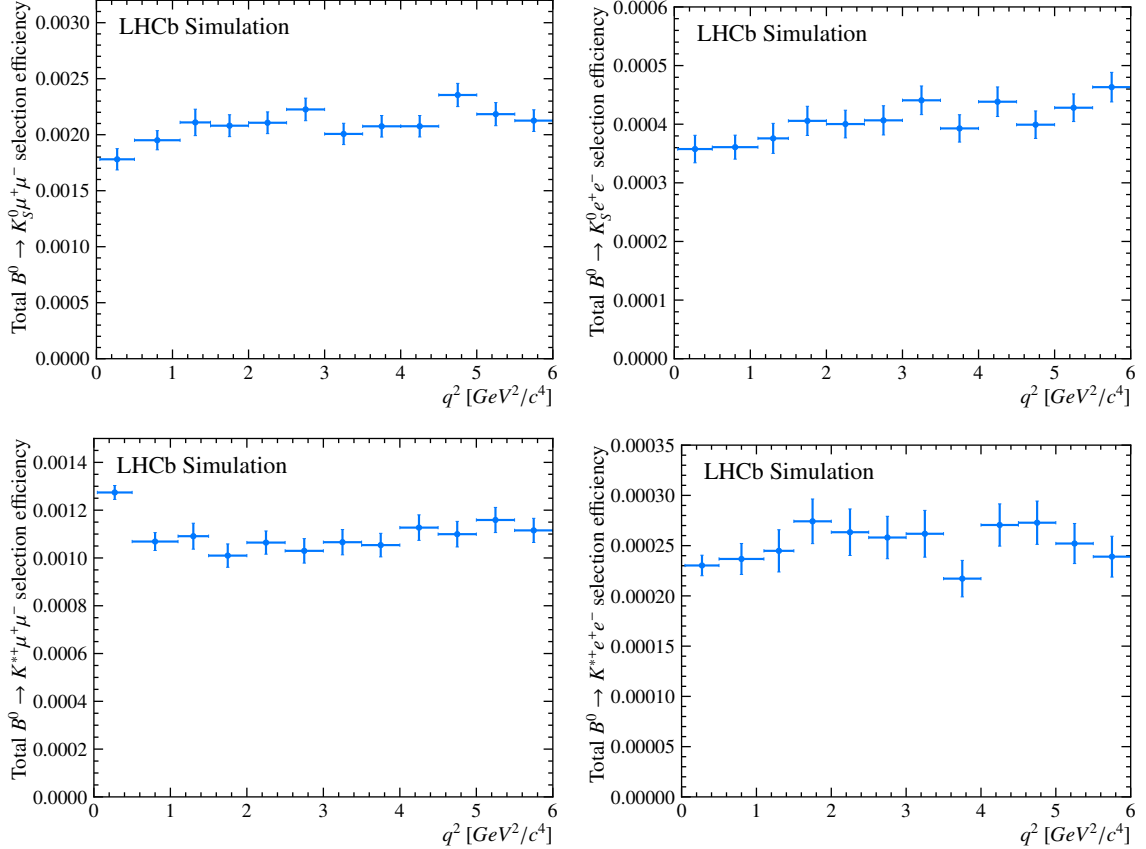


Figure 3: Total selection efficiencies as a function of q^2 , for (top left) $B^0 \rightarrow K_S^0 \mu^+ \mu^-$, (top right) $B^0 \rightarrow K_S^0 e^+ e^-$, (bottom left) $B^+ \rightarrow K^{*+} \mu^+ \mu^-$, and (bottom right) $B^+ \rightarrow K^{*+} e^+ e^-$ decays. The efficiencies are evaluated using simulated candidates that have been corrected to improve agreement with data. These efficiencies account for detector resolution effects including the effect of bremsstrahlung, which may cause a candidate to be reconstructed in a different bin of q^2 than would be dictated by its ‘true’ value.

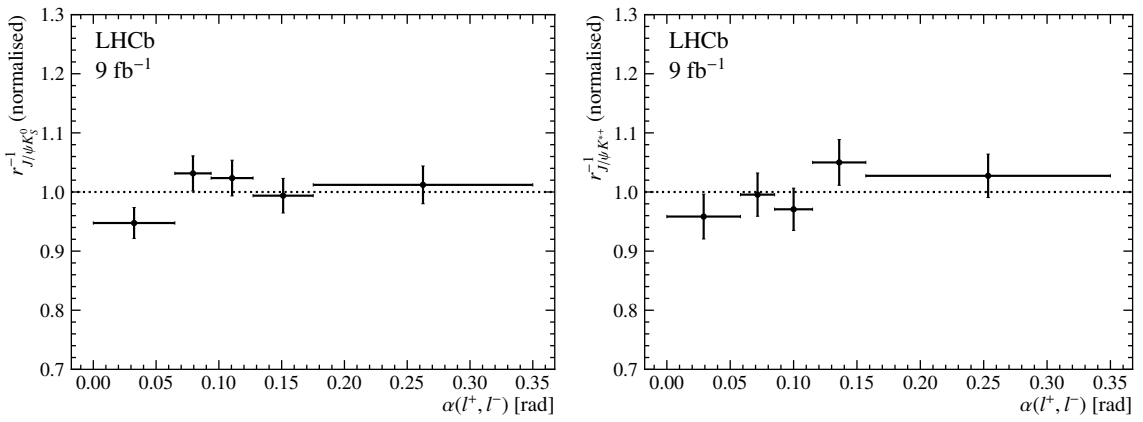


Figure 4: Single ratios (left) $r_{J/\psi K_S^0}^{-1}$ and (right) $r_{J/\psi K^{*+}}^{-1}$ as a function of the opening angle of the two leptons, normalised to their average value.

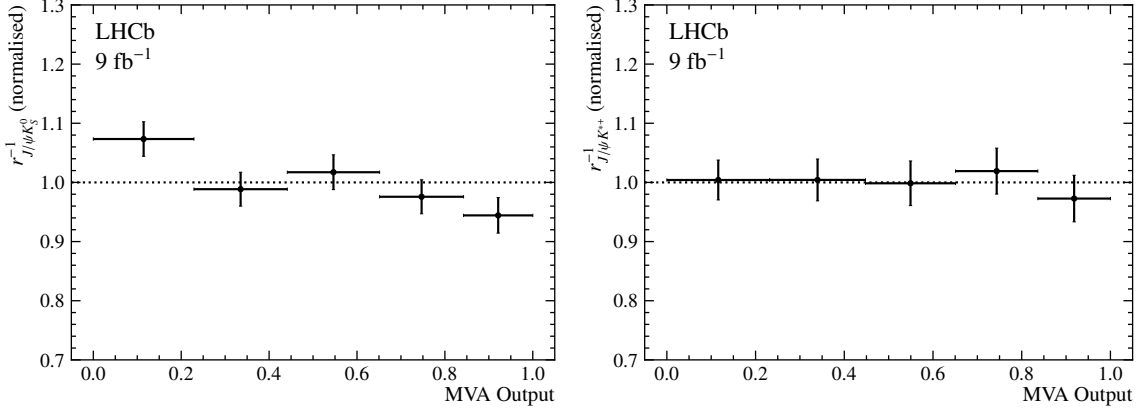


Figure 5: Single ratios (left) $r_{J/\psi K_S^0}^{-1}$ and (right) $r_{J/\psi K^{*+}}^{-1}$ as a function of the output of an MVA trained to separate the signal and control modes, normalised to their average value.

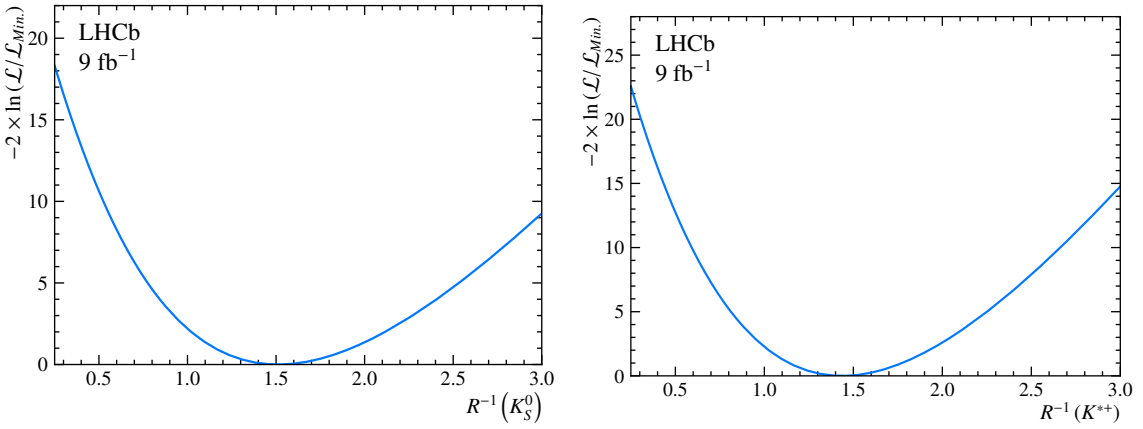


Figure 6: Scans of the profile likelihoods as a function of (left) $R_{K_S^0}^{-1}$, and (right) $R_{K^{*+}}^{-1}$.

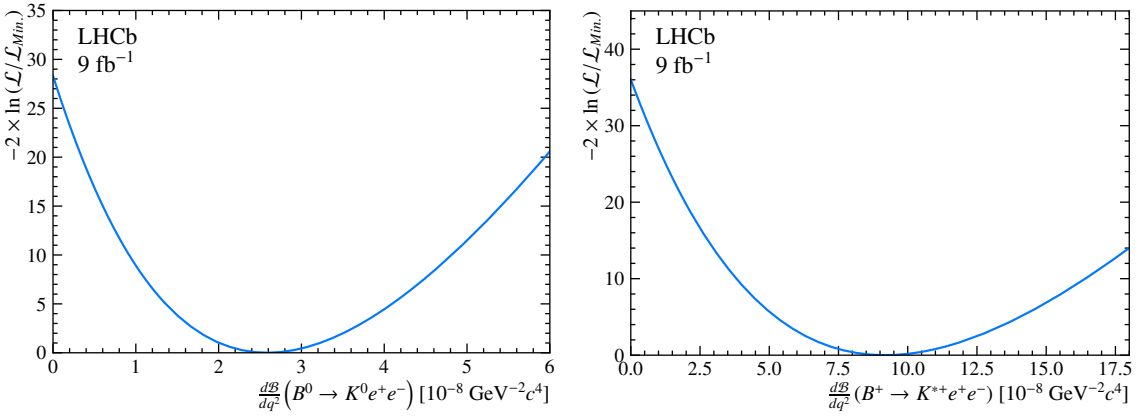


Figure 7: Scans of the profile likelihoods as a function of the differential branching fractions for (left) $B^0 \rightarrow K^0 e^+ e^-$ decays, and (right) $B^+ \rightarrow K^{*+} e^+ e^-$ decays.

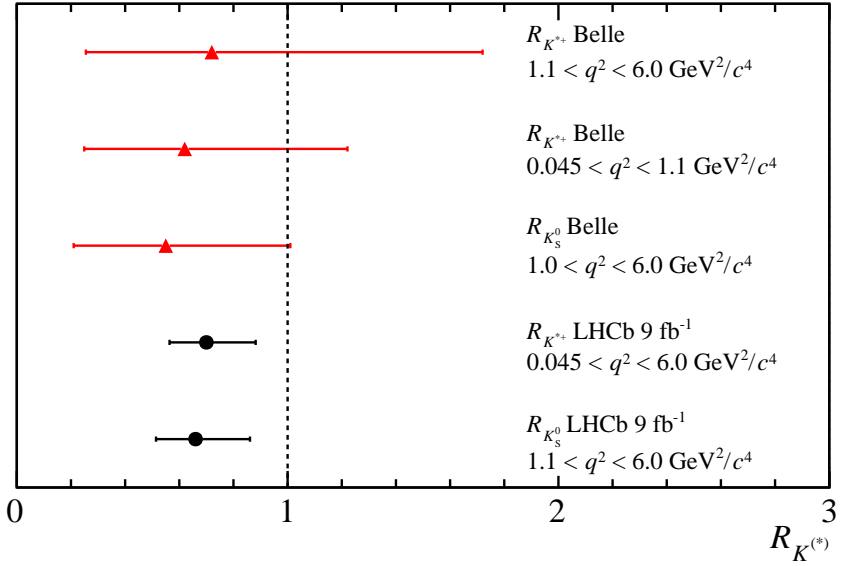


Figure 8: Measurements of $R_{K_S^0}$ and $R_{K^{*+}}$ performed by the LHCb and Belle collaborations [101, 102].

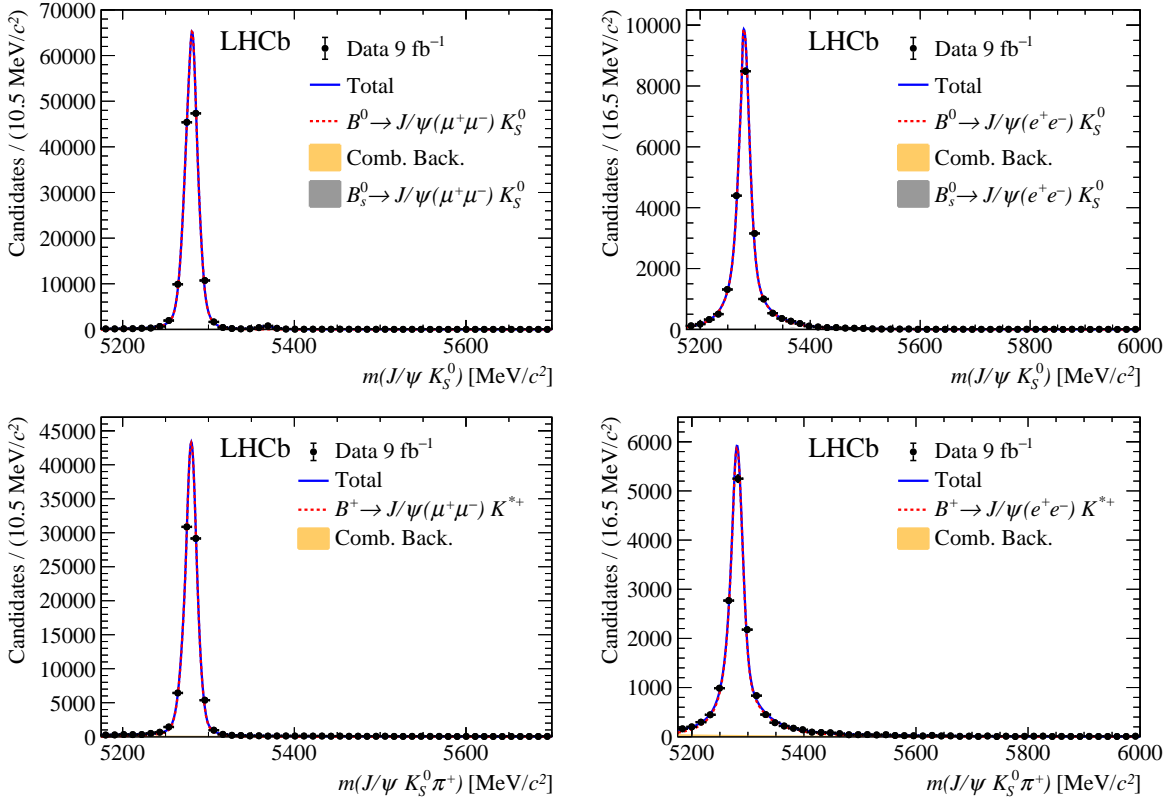


Figure 9: Distributions of (top left) $J/\psi(\mu^+\mu^-)K_S^0$ mass, (top right) $J/\psi(e^+e^-)K_S^0$ mass, (bottom left) $J/\psi(\mu^+\mu^-)K_S^0\pi^+$ mass and (bottom right) $J/\psi(e^+e^-)K_S^0\pi^+$ mass with the fit models used to determine the control mode yields.

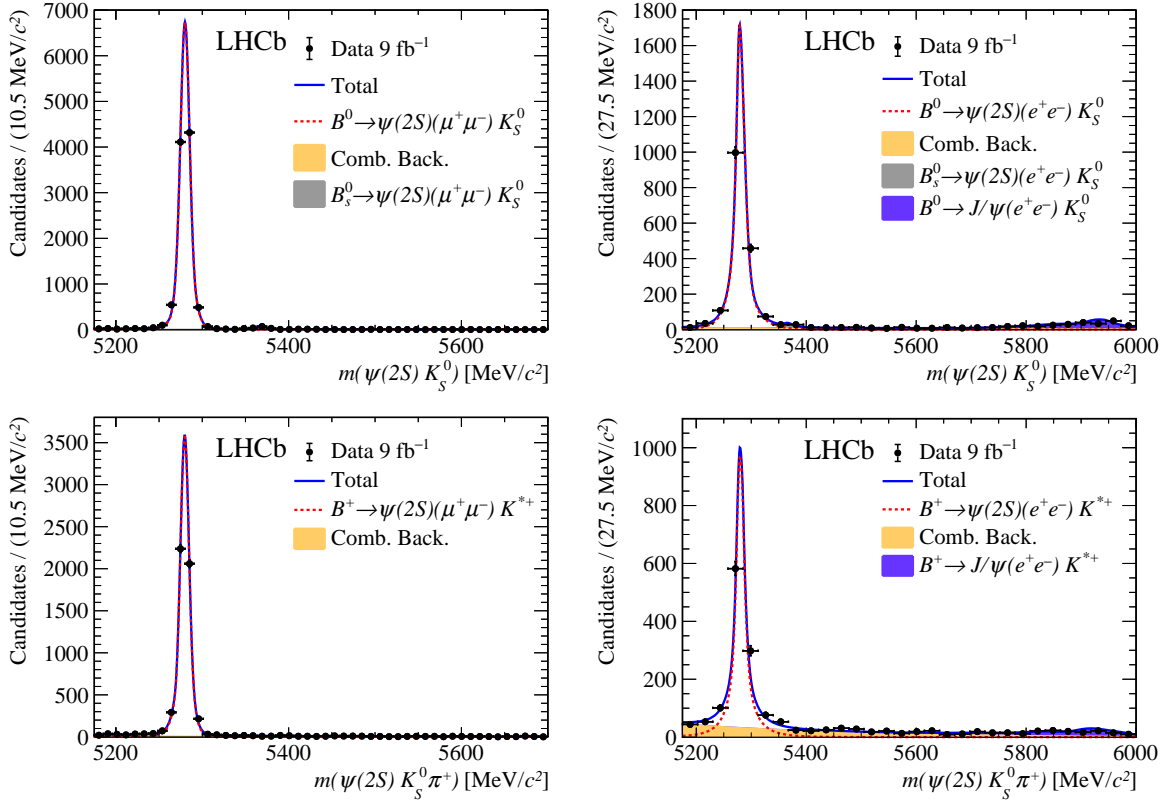


Figure 10: Distributions of (top left) $\psi(2S)(\mu^+\mu^-)K_S^0$ mass, (top right) $\psi(2S)(e^+e^-)K_S^0$ mass, (bottom left) $\psi(2S)(\mu^+\mu^-)K_S^0\pi^+$ mass and (bottom right) $\psi(2S)(e^+e^-)K_S^0\pi^+$ mass with the fit models used to determine the $\psi(2S)$ control mode yields.

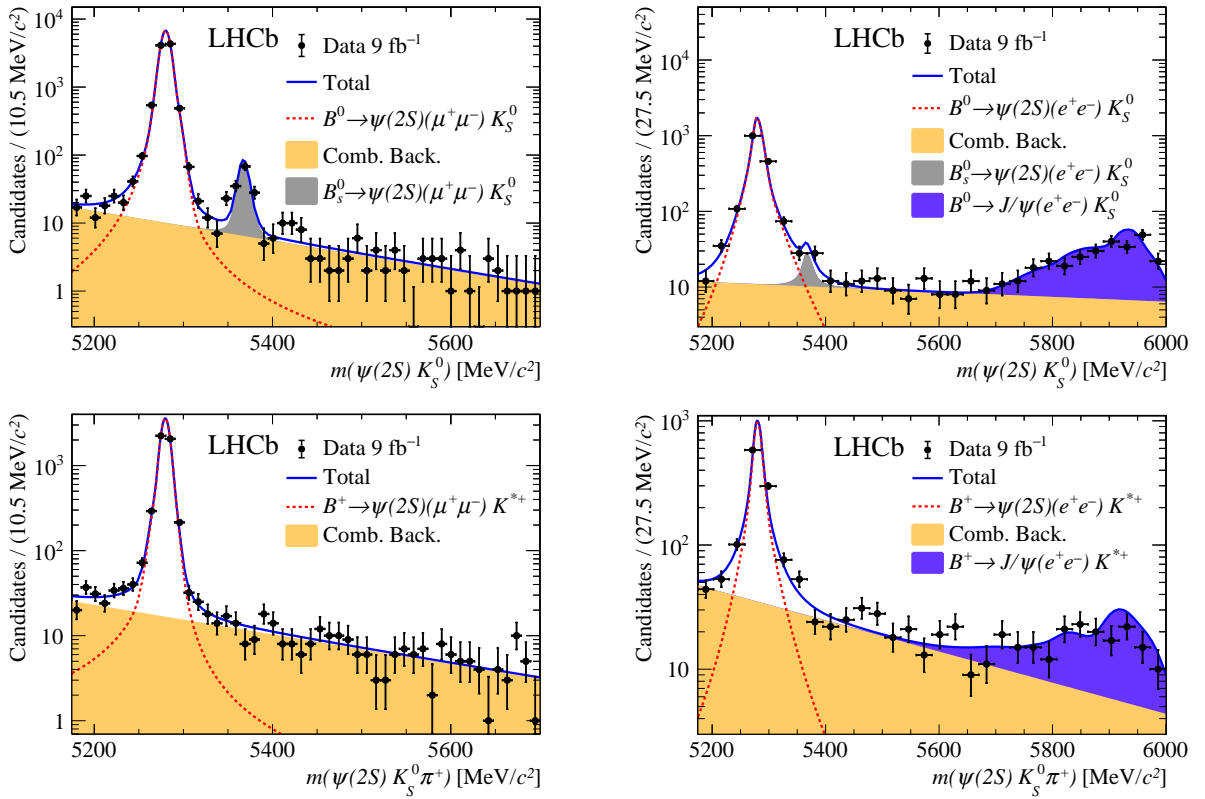


Figure 11: Distributions of (top left) $\psi(2S)(\mu^+\mu^-)K_S^0$ mass, (top right) $\psi(2S)(e^+e^-)K_S^0$ mass, (bottom left) $\psi(2S)(\mu^+\mu^-)K_S^0\pi^+$ mass and (bottom right) $\psi(2S)(e^+e^-)K_S^0\pi^+$ mass with the fit models used to determine the $\psi(2S)$ control mode yields.

References

- [1] G. Hiller and F. Krüger, *More model-independent analysis of $b \rightarrow s$ processes*, Phys. Rev. **D69** (2004) 074020, [arXiv:hep-ph/0310219](#).
- [2] M. Bordone, G. Isidori, and A. Pattori, *On the Standard Model predictions for R_K and R_{K^*}* , Eur. Phys. J. **C76** (2016) 440, [arXiv:1605.07633](#).
- [3] G. Isidori, S. Nabebaccus, and R. Zwicky, *QED corrections in $\bar{B} \rightarrow \bar{K}\ell^+\ell^-$ at the double-differential level*, JHEP **12** (2020) 104, [arXiv:2009.00929](#).
- [4] C. Bobeth, G. Hiller, and G. Piranishvili, *Angular distributions of $\bar{B} \rightarrow \bar{K}\ell^+\ell^-$ decays*, JHEP **12** (2007) 040, [arXiv:0709.4174](#).
- [5] LHCb collaboration, R. Aaij *et al.*, *Test of lepton universality with $B^0 \rightarrow K^{*0}\ell^+\ell^-$ decays*, JHEP **08** (2017) 055, [arXiv:1705.05802](#).
- [6] LHCb collaboration, R. Aaij *et al.*, *Test of lepton universality in beauty-quark decays*, Nature Phys. **18** (2022) 277, [arXiv:2103.11769](#).
- [7] LHCb collaboration, R. Aaij *et al.*, *Test of lepton universality using $\Lambda_b^0 \rightarrow p K^-\ell^+\ell^-$ decays*, JHEP **05** (2020) 040, [arXiv:1912.08139](#).
- [8] LHCb collaboration, R. Aaij *et al.*, *Angular analysis of the $B^+ \rightarrow K^{*+}\mu^+\mu^-$ decay*, Phys. Rev. Lett. **126** (2021) 161802, [arXiv:2012.13241](#).
- [9] LHCb collaboration, R. Aaij *et al.*, *Measurement of CP-averaged observables in the $B^0 \rightarrow K^{*0}\mu^+\mu^-$ decay*, Phys. Rev. Lett. **125** (2020) 011802, [arXiv:2003.04831](#).
- [10] LHCb collaboration, R. Aaij *et al.*, *Angular analysis of the $B^0 \rightarrow K^{*0}\mu^+\mu^-$ decay using 3 fb^{-1} of integrated luminosity*, JHEP **02** (2016) 104, [arXiv:1512.04442](#).
- [11] LHCb collaboration, R. Aaij *et al.*, *Angular analysis of the rare decay $B_s^0 \rightarrow \phi\mu^+\mu^-$* , JHEP **11** (2021) 043, [arXiv:2107.13428](#).
- [12] ATLAS collaboration, M. Aaboud *et al.*, *Angular analysis of $B_d^0 \rightarrow K^*\mu^+\mu^-$ decays in pp collisions at $\sqrt{s} = 8$ TeV with the ATLAS detector*, JHEP **10** (2018) 047, [arXiv:1805.04000](#).
- [13] BaBar collaboration, B. Aubert *et al.*, *Measurements of branching fractions, rate asymmetries, and angular distributions in the rare decays $B \rightarrow K\ell^+\ell^-$ and $B \rightarrow K^*\ell^+\ell^-$* , Phys. Rev. **D73** (2006) 092001, [arXiv:hep-ex/0604007](#).
- [14] BaBar collaboration, J. P. Lees *et al.*, *Measurement of angular asymmetries in the decays $B \rightarrow K^*\ell^+\ell^-$* , Phys. Rev. **D93** (2016) 052015, [arXiv:1508.07960](#).
- [15] Belle collaboration, J.-T. Wei *et al.*, *Measurement of the differential branching Fraction and forward-backward Asymmetry for $B \rightarrow K^{(*)}\ell^+\ell^-$* , Phys. Rev. Lett. **103** (2009) 171801, [arXiv:0904.0770](#).
- [16] Belle collaboration, S. Wehle *et al.*, *Lepton-flavor-dependent angular analysis of $B \rightarrow K^*\ell^+\ell^-$* , Phys. Rev. Lett. **118** (2017) 111801, [arXiv:1612.05014](#).

- [17] CDF collaboration, T. Aaltonen *et al.*, *Measurements of the angular distributions in the decays $B \rightarrow K^{(*)}\mu^+\mu^-$ at CDF*, Phys. Rev. Lett. **108** (2012) 081807, [arXiv:1108.0695](#).
- [18] CMS collaboration, V. Khachatryan *et al.*, *Angular analysis of the decay $B^0 \rightarrow K^{*0}\mu^+\mu^-$ from pp collisions at $\sqrt{s} = 8$ TeV*, Phys. Lett. **B753** (2016) 424, [arXiv:1507.08126](#).
- [19] CMS collaboration, A. M. Sirunyan *et al.*, *Measurement of angular parameters from the decay $B^0 \rightarrow K^{*0}\mu^+\mu^-$ in proton-proton collisions at $\sqrt{s} = 8$ TeV*, Phys. Lett. **B781** (2018) 517, [arXiv:1710.02846](#).
- [20] LHCb collaboration, R. Aaij *et al.*, *Measurements of the S-wave fraction in $B^0 \rightarrow K^+\pi^-\mu^+\mu^-$ decays and the $B^0 \rightarrow K^*(892)^0\mu^+\mu^-$ differential branching fraction*, JHEP **11** (2016) 047, Erratum *ibid.* **04** (2017) 142, [arXiv:1606.04731](#).
- [21] LHCb collaboration, R. Aaij *et al.*, *Branching fraction measurements of the rare $B_s^0 \rightarrow \phi\mu^+\mu^-$ and $B_s^0 \rightarrow f'_2(1525)\mu^+\mu^-$ decays*, Phys. Rev. Lett. **127** (2021) 151801, [arXiv:2105.14007](#).
- [22] LHCb collaboration, R. Aaij *et al.*, *Differential branching fractions and isospin asymmetries of $B \rightarrow K^{(*)}\mu^+\mu^-$ decays*, JHEP **06** (2014) 133, [arXiv:1403.8044](#).
- [23] LHCb collaboration, R. Aaij *et al.*, *Differential branching fraction and angular analysis of $\Lambda_b^0 \rightarrow \Lambda\mu^+\mu^-$ decays*, JHEP **06** (2015) 115, Erratum *ibid.* **09** (2018) 145, [arXiv:1503.07138](#).
- [24] S. Descotes-Genon, L. Hofer, J. Matias, and J. Virto, *Global analysis of $b \rightarrow s\ell\ell$ anomalies*, JHEP **06** (2016) 092, [arXiv:1510.04239](#).
- [25] S. Jäger and J. Martin Camalich, *Reassessing the discovery potential of the $B \rightarrow K^*\ell^+\ell^-$ decays in the large-recoil region: SM challenges and BSM opportunities*, Phys. Rev. **D93** (2016) 014028, [arXiv:1412.3183](#).
- [26] J. Lyon and R. Zwicky, *Resonances gone topsy turvy - the charm of QCD or new physics in $b \rightarrow s\ell^+\ell^-$?*, [arXiv:1406.0566](#).
- [27] A. Khodjamirian, T. Mannel, and Y. M. Wang, *$B \rightarrow K\ell^+\ell^-$ decay at large hadronic recoil*, JHEP **02** (2013) 010, [arXiv:1211.0234](#).
- [28] A. Khodjamirian, T. Mannel, A. A. Pivovarov, and Y.-M. Wang, *Charm-loop effect in $B \rightarrow K^{(*)}\ell^+\ell^-$ and $B \rightarrow K^*\gamma$* , JHEP **09** (2010) 089, [arXiv:1006.4945](#).
- [29] S. Descotes-Genon, L. Hofer, J. Matias, and J. Virto, *On the impact of power corrections in the prediction of $B \rightarrow K^*\mu^+\mu^-$ observables*, JHEP **12** (2014) 125, [arXiv:1407.8526](#).
- [30] R. R. Horgan, Z. Liu, S. Meinel, and M. Wingate, *Calculation of $B^0 \rightarrow K^{*0}\mu^+\mu^-$ and $B_s^0 \rightarrow \phi\mu^+\mu^-$ observables using form factors from lattice QCD*, Phys. Rev. Lett. **112** (2014) 212003, [arXiv:1310.3887](#).

- [31] F. Beaujean, C. Bobeth, and D. van Dyk, *Comprehensive Bayesian analysis of rare (semi)leptonic and radiative B decays*, Eur. Phys. J. **C74** (2014) 2897, Erratum ibid. **C74** (2014) 3179, [arXiv:1310.2478](#).
- [32] C. Hambrock, G. Hiller, S. Schacht, and R. Zwicky, *$B \rightarrow K^*$ form factors from flavor data to QCD and back*, Phys. Rev. **D89** (2014) 074014, [arXiv:1308.4379](#).
- [33] W. Altmannshofer and D. M. Straub, *New physics in $B \rightarrow K^*\mu\mu?$* , Eur. Phys. J. **C73** (2013) 2646, [arXiv:1308.1501](#).
- [34] C. Bobeth, M. Chrzaszcz, D. van Dyk, and J. Virto, *Long-distance effects in $B \rightarrow K^*\ell\ell$ from analyticity*, Eur. Phys. J. **C78** (2018) 451, [arXiv:1707.07305](#).
- [35] M. Ciuchini *et al.*, *Lessons from the $B^{0,+} \rightarrow K^{*,0,+}\mu^+\mu^-$ angular analyses*, Phys. Rev. **D103** (2021) 015030, [arXiv:2011.01212](#).
- [36] K. Kowalska, D. Kumar, and E. M. Sessolo, *Implications for new physics in $b \rightarrow s\mu\mu$ transitions after recent measurements by Belle and LHCb*, Eur. Phys. J. **C79** (2019) 840, [arXiv:1903.10932](#).
- [37] M. Algueró *et al.*, *Emerging patterns of new physics with and without lepton flavour universal contributions*, Eur. Phys. J. **C79** (2019) 714, Addendum ibid. **C80** (2020) 511, [arXiv:1903.09578](#).
- [38] T. Hurth, F. Mahmoudi, and S. Neshatpour, *Implications of the new LHCb angular analysis of $B \rightarrow K^*\mu^+\mu^-$: Hadronic effects or new physics?*, Phys. Rev. **D102** (2020) 055001, [arXiv:2006.04213](#).
- [39] M. Ciuchini *et al.*, *New physics in $b \rightarrow s\ell^+\ell^-$ confronts new data on lepton universality*, Eur. Phys. J. **C79** (2019) 719, [arXiv:1903.09632](#).
- [40] J. Aebischer *et al.*, *B -decay discrepancies after Moriond 2019*, Eur. Phys. J. **C80** (2020) 252, [arXiv:1903.10434](#).
- [41] A. K. Alok, A. Dighe, S. Gangal, and D. Kumar, *Continuing search for new physics in $b \rightarrow s\mu\mu$ decays: two operators at a time*, JHEP **06** (2019) 089, [arXiv:1903.09617](#).
- [42] W. Altmannshofer and P. Stangl, *New physics in rare B decays after Moriond 2021*, Eur. Phys. J. C **81** (2021) 952, [arXiv:2103.13370](#).
- [43] L.-S. Geng *et al.*, *Implications of new evidence for lepton-universality violation in brightarrowsl $^+\ell^-$ decays*, Phys. Rev. **D104** (2021) 035029, [arXiv:2103.12738](#).
- [44] C. Cornella *et al.*, *Reading the footprints of the B -meson flavor anomalies*, JHEP **08** (2021) 050, [arXiv:2103.16558](#).
- [45] M. Algueró *et al.*, *$b \rightarrow s\ell\ell$ global fits after Moriond 2021 results*, in *55th Rencontres de Moriond on QCD and High Energy Interactions*, 2021, [arXiv:2104.08921](#).
- [46] T. Hurth, F. Mahmoudi, D. M. Santos, and S. Neshatpour, *More indications for lepton nonuniversality in $b \rightarrow s\ell^+\ell^-$* , Phys. Lett. B **824** (2022) 136838, [arXiv:2104.10058](#).

- [47] W. Altmannshofer, S. Gori, M. Pospelov, and I. Yavin, *Quark flavor transitions in $L_\mu - L_\tau$ models*, Phys. Rev. **D89** (2014) 095033, [arXiv:1403.1269](#).
- [48] A. Crivellin, G. D'Ambrosio, and J. Heeck, *Explaining $h \rightarrow \mu^\pm \tau^\mp$, $B \rightarrow K^* \mu^+ \mu^-$ and $B \rightarrow K \mu^+ \mu^- / B \rightarrow K e^+ e^-$ in a two-Higgs-doublet model with gauged $L_\mu - L_\tau$* , Phys. Rev. Lett. **114** (2015) 151801, [arXiv:1501.00993](#).
- [49] A. Celis, J. Fuentes-Martin, M. Jung, and H. Serodio, *Family nonuniversal Z' models with protected flavor-changing interactions*, Phys. Rev. **D92** (2015) 015007, [arXiv:1505.03079](#).
- [50] A. Falkowski, M. Nardecchia, and R. Ziegler, *Lepton flavor non-universality in B -meson decays from a $U(2)$ flavor model*, JHEP **11** (2015) 173, [arXiv:1509.01249](#).
- [51] B. C. Allanach, J. M. Butterworth, and T. Corbett, *Collider constraints on Z' models for neutral current B -anomalies*, JHEP **08** (2019) 106, [arXiv:1904.10954](#).
- [52] B. C. Allanach and J. Davighi, *Naturalising the third family hypercharge model for neutral current B -anomalies*, Eur. Phys. J. **C79** (2019) 908, [arXiv:1905.10327](#).
- [53] J. Kawamura, S. Raby, and A. Trautner, *Complete vectorlike fourth family and new $U(1)'$ for muon anomalies*, Phys. Rev. **D100** (2019) 055030, [arXiv:1906.11297](#).
- [54] S. Dwivedi, D. Kumar Ghosh, A. Falkowski, and N. Ghosh, *Associated Z' production in the flavorful $U(1)$ scenario for $R_{K^{(*)}}$* , Eur. Phys. J. **C80** (2020) 263, [arXiv:1908.03031](#).
- [55] Z.-L. Han, R. Ding, S.-J. Lin, and B. Zhu, *Gauged $U(1)_{L_\mu - L_\tau}$ scotogenic model in light of $R_{K^{(*)}}$ anomaly and AMS-02 positron excess*, Eur. Phys. J. **C79** (2019) 1007, [arXiv:1908.07192](#).
- [56] B. Capdevila, A. Crivellin, C. A. Manzari, and M. Montull, *Explaining $b \rightarrow s \ell^+ \ell^-$ and the Cabibbo angle anomaly with a vector triplet*, Phys. Rev. **D103** (2021) 015032, [arXiv:2005.13542](#).
- [57] W. Altmannshofer, J. Davighi, and M. Nardecchia, *Gauging the accidental symmetries of the standard model, and implications for the flavor anomalies*, Phys. Rev. **D101** (2020) 015004, [arXiv:1909.02021](#).
- [58] S.-L. Chen *et al.*, *Signatures of a flavor changing Z' boson in $B_q \rightarrow \gamma Z'$* , Nucl. Phys. **B962** (2021) 115237, [arXiv:2006.03383](#).
- [59] A. Carvunis, D. Guadagnoli, M. Reboud, and P. Stangl, *Composite dark matter and a horizontal symmetry*, JHEP **02** (2021) 056, [arXiv:2007.11931](#).
- [60] A. Karozas, G. K. Leontaris, I. Tavellaris, and N. D. Vlachos, *On the LHC signatures of $SU(5) \times U(1)'$ F-theory motivated models*, Eur. Phys. J. **C81** (2021) 35, [arXiv:2007.05936](#).
- [61] D. Borah, L. Mukherjee, and S. Nandi, *Low scale $U(1)_X$ gauge symmetry as an origin of dark matter, neutrino mass and flavour anomalies*, JHEP **12** (2020) 052, [arXiv:2007.13778](#).

- [62] B. C. Allanach, *$U(1)_{B_3-L_2}$ explanation of the neutral current B -anomalies*, Eur. Phys. J. **C81** (2021) 56, Erratum ibid. **C81** (2021) 321, [arXiv:2009.02197](#).
- [63] J.-H. Sheng, *The analysis of $b \rightarrow s\ell^+\ell^-$ in the family non-universal Z' model*, Int. J. Theor. Phys. **60** (2021) 26.
- [64] G. Hiller and M. Schmaltz, *R_K and future $b \rightarrow s\ell\ell$ physics beyond the standard model opportunities*, Phys. Rev. **D90** (2014) 054014, [arXiv:1408.1627](#).
- [65] L. Di Luzio, A. Greljo, and M. Nardecchia, *Gauge leptoquark as the origin of B -physics anomalies*, Phys. Rev. **D96** (2017) 115011, [arXiv:1708.08450](#).
- [66] A. Greljo and B. A. Stefanek, *Third family quark-lepton unification at the TeV scale*, Phys. Lett. **B782** (2018) 131, [arXiv:1802.04274](#).
- [67] B. Gripaios, M. Nardecchia, and S. A. Renner, *Composite leptoquarks and anomalies in B -meson decays*, JHEP **05** (2015) 006, [arXiv:1412.1791](#).
- [68] I. de Medeiros Varzielas and G. Hiller, *Clues for flavor from rare lepton and quark decays*, JHEP **06** (2015) 072, [arXiv:1503.01084](#).
- [69] R. Barbieri, C. W. Murphy, and F. Senia, *B -decay anomalies in a composite leptoquark model*, Eur. Phys. J. **C77** (2017) 8, [arXiv:1611.04930](#).
- [70] M. Bordone, C. Cornella, J. Fuentes-Martín, and G. Isidori, *Low-energy signatures of the PS³ model: from B -physics anomalies to LFV*, JHEP **10** (2018) 148, [arXiv:1805.09328](#).
- [71] B. Fornal, S. A. Gadom, and B. Grinstein, *Left-right $SU(4)$ vector leptoquark model for flavor anomalies*, Phys. Rev. **D99** (2019) 055025, [arXiv:1812.01603](#).
- [72] S. Balaji and M. A. Schmidt, *Unified $SU(4)$ theory for the $R_{D^{(*)}}$ and $R_{K^{(*)}}$ anomalies*, Phys. Rev. **D101** (2020) 015026, [arXiv:1911.08873](#).
- [73] C. Cornella, J. Fuentes-Martin, and G. Isidori, *Revisiting the vector leptoquark explanation of the B -physics anomalies*, JHEP **07** (2019) 168, [arXiv:1903.11517](#).
- [74] A. Datta, D. Sachdeva, and J. Waite, *Unified explanation of $b \rightarrow s\mu^+\mu^-$ anomalies, neutrino masses, and $B \rightarrow \pi K$ puzzle*, Phys. Rev. **D100** (2019) 055015, [arXiv:1905.04046](#).
- [75] O. Popov, M. A. Schmidt, and G. White, *R_2 as a single leptoquark solution to $R_{D^{(*)}}$ and $R_{K^{(*)}}$* , Phys. Rev. **D100** (2019) 035028, [arXiv:1905.06339](#).
- [76] I. Bigaran, J. Gargalionis, and R. R. Volkas, *A near-minimal leptoquark model for reconciling flavour anomalies and generating radiative neutrino masses*, JHEP **10** (2019) 106, [arXiv:1906.01870](#).
- [77] J. Bernigaud, I. de Medeiros Varzielas, and J. Talbert, *Finite family groups for fermionic and leptoquark mixing patterns*, JHEP **01** (2020) 194, [arXiv:1906.11270](#).
- [78] L. Da Rold and F. Lamagna, *A vector leptoquark for the B -physics anomalies from a composite GUT*, JHEP **12** (2019) 112, [arXiv:1906.11666](#).

- [79] J. Fuentes-Martín, M. Reig, and A. Vicente, *Strong CP problem with low-energy emergent QCD: The 4321 case*, Phys. Rev. **D100** (2019) 115028, [arXiv:1907.02550](#).
- [80] C. Hati, J. Kriewald, J. Orloff, and A. M. Teixeira, *A nonunitary interpretation for a single vector leptoquark combined explanation to the B-decay anomalies*, JHEP **12** (2019) 006, [arXiv:1907.05511](#).
- [81] A. Datta, J. L. Feng, S. Kamali, and J. Kumar, *Resolving the $(g - 2)_\mu$ and B anomalies with leptoquarks and a dark Higgs boson*, Phys. Rev. **D101** (2020) 035010, [arXiv:1908.08625](#).
- [82] A. Crivellin, D. Müller, and F. Saturnino, *Flavor phenomenology of the leptoquark singlet-triplet model*, JHEP **06** (2020) 020, [arXiv:1912.04224](#).
- [83] C. Borschensky, B. Fuks, A. Kulesza, and D. Schwartländer, *Scalar leptoquark pair production at hadron colliders*, Phys. Rev. **D101** (2020) 115017, [arXiv:2002.08971](#).
- [84] S. Saad, *Combined explanations of $(g - 2)_\mu$, $R_{D^{(*)}}$, $R_{K^{(*)}}$ anomalies in a two-loop radiative neutrino mass model*, Phys. Rev. **D102** (2020) 015019, [arXiv:2005.04352](#).
- [85] J. Fuentes-Martín and P. Stangl, *Third-family quark-lepton unification with a fundamental composite Higgs*, Phys. Lett. **B811** (2020) 135953, [arXiv:2004.11376](#).
- [86] P. S. Bhupal Dev, R. Mohanta, S. Patra, and S. Sahoo, *Unified explanation of flavor anomalies, radiative neutrino masses, and ANITA anomalous events in a vector leptoquark model*, Phys. Rev. **D102** (2020) 095012, [arXiv:2004.09464](#).
- [87] B. Fornal, *Gravitational wave signatures of lepton universality violation*, Phys. Rev. **D103** (2021) 015018, [arXiv:2006.08802](#).
- [88] J. Davighi, M. Kirk, and M. Nardecchia, *Anomalies and accidental symmetries: charging the scalar leptoquark under $L_\mu - L_\tau$* , JHEP **12** (2020) 111, [arXiv:2007.15016](#).
- [89] K. S. Babu, P. S. B. Dev, S. Jana, and A. Thapa, *Unified framework for B-anomalies, muon $g - 2$ and neutrino masses*, JHEP **03** (2021) 179, [arXiv:2009.01771](#).
- [90] A. Angelescu *et al.*, *Single leptoquark solutions to the B-physics anomalies*, Phys. Rev. **D104** (2021) 055017, [arXiv:2103.12504](#).
- [91] S. Trifinopoulos, *B -physics anomalies: The bridge between R -parity violating supersymmetry and flavored dark matter*, Phys. Rev. **D100** (2019) 115022, [arXiv:1904.12940](#).
- [92] Q.-Y. Hu and L.-L. Huang, *Explaining $b \rightarrow s\ell^+\ell^-$ data by sneutrinos in the R -parity violating MSSM*, Phys. Rev. **D101** (2020) 035030, [arXiv:1912.03676](#).
- [93] Q.-Y. Hu, Y.-D. Yang, and M.-D. Zheng, *Revisiting the B-physics anomalies in R-parity violating MSSM*, Eur. Phys. J. **C80** (2020) 365, [arXiv:2002.09875](#).
- [94] A. Shaw, *Looking for $B \rightarrow X_s\ell^+\ell^-$ in a nonminimal universal extra dimensional model*, Phys. Rev. **D99** (2019) 115030, [arXiv:1903.10302](#).

- [95] B. Barman, D. Borah, L. Mukherjee, and S. Nandi, *Correlating the anomalous results in $b \rightarrow s$ decays with inert Higgs doublet dark matter and muon $(g - 2)$* , Phys. Rev. **D100** (2019) 115010, [arXiv:1808.06639](#).
- [96] P. Arnan, A. Crivellin, M. Fedele, and F. Mescia, *Generic loop effects of new scalars and fermions in $b \rightarrow sl^+l^-$, $(g - 2)_\mu$ and a vector-like 4th generation*, JHEP **06** (2019) 118, [arXiv:1904.05890](#).
- [97] L. Delle Rose, S. Khalil, S. J. D. King, and S. Moretti, *R_K and R_{K^*} in an aligned 2HDM with right-handed neutrinos*, Phys. Rev. **D101** (2020) 115009, [arXiv:1903.11146](#).
- [98] A. Ordell, R. Pasechnik, H. Serôdio, and F. Nottensteiner, *Classification of anomaly-free 2HDMs with a gauged U(1)' symmetry*, Phys. Rev. **D100** (2019) 115038, [arXiv:1909.05548](#).
- [99] C. Marzo, L. Marzola, and M. Raidal, *Common explanation to the $R_{K^{(*)}}$, $R_{D^{(*)}}$ and ϵ'/ϵ anomalies in a 3HDM+ ν_R and connections to neutrino physics*, Phys. Rev. **D100** (2019) 055031, [arXiv:1901.08290](#).
- [100] BaBar collaboration, J. P. Lees *et al.*, *Measurement of branching fractions and rate asymmetries in the rare decays $B \rightarrow K^{(*)}l^+l^-$* , Phys. Rev. **D86** (2012) 032012, [arXiv:1204.3933](#).
- [101] Belle collaboration, A. Abdesselam *et al.*, *Test of lepton-flavor universality in $B \rightarrow K^*\ell^+\ell^-$ decays at Belle*, Phys. Rev. Lett. **126** (2021) 161801, [arXiv:1904.02440](#).
- [102] Belle collaboration, S. Choudhury *et al.*, *Test of lepton flavor universality and search for lepton flavor violation in $B \rightarrow K\ell\ell$ decays*, JHEP **03** (2021) 105, [arXiv:1908.01848](#).
- [103] Particle Data Group, P. A. Zyla *et al.*, *Review of particle physics*, Prog. Theor. Exp. Phys. **2020** (2020) 083C01.
- [104] LHCb collaboration, A. A. Alves Jr. *et al.*, *The LHCb detector at the LHC*, JINST **3** (2008) S08005.
- [105] LHCb collaboration, R. Aaij *et al.*, *LHCb detector performance*, Int. J. Mod. Phys. **A30** (2015) 1530022, [arXiv:1412.6352](#).
- [106] T. Sjöstrand, S. Mrenna, and P. Skands, *A brief introduction to PYTHIA 8.1*, Comput. Phys. Commun. **178** (2008) 852, [arXiv:0710.3820](#); T. Sjöstrand, S. Mrenna, and P. Skands, *PYTHIA 6.4 physics and manual*, JHEP **05** (2006) 026, [arXiv:hep-ph/0603175](#).
- [107] I. Belyaev *et al.*, *Handling of the generation of primary events in Gauss, the LHCb simulation framework*, J. Phys. Conf. Ser. **331** (2011) 032047.
- [108] D. J. Lange, *The EvtGen particle decay simulation package*, Nucl. Instrum. Meth. **A462** (2001) 152.

- [109] Geant4 collaboration, J. Allison *et al.*, *Geant4 developments and applications*, IEEE Trans. Nucl. Sci. **53** (2006) 270; Geant4 collaboration, S. Agostinelli *et al.*, *Geant4: A simulation toolkit*, Nucl. Instrum. Meth. **A506** (2003) 250.
- [110] M. Clemencic *et al.*, *The LHCb simulation application, Gauss: Design, evolution and experience*, J. Phys. Conf. Ser. **331** (2011) 032023.
- [111] N. Davidson, T. Przedzinski, and Z. Was, *PHOTOS interface in C++: Technical and physics documentation*, Comp. Phys. Comm. **199** (2016) 86, [arXiv:1011.0937](https://arxiv.org/abs/1011.0937).
- [112] BaBar collaboration, B. Aubert *et al.*, *Measurement of branching fractions and charge asymmetries for exclusive B decays to charmonium*, Phys. Rev. Lett. **94** (2005) 141801, [arXiv:hep-ex/0412062](https://arxiv.org/abs/hep-ex/0412062).
- [113] Belle collaboration, K. Abe *et al.*, *Measurements of branching fractions and decay amplitudes in $B \rightarrow J/\psi K^*$ decays*, Phys. Lett. **B538** (2002) 11, [arXiv:hep-ex/0205021](https://arxiv.org/abs/hep-ex/0205021).
- [114] L. Breiman, J. H. Friedman, R. A. Olshen, and C. J. Stone, *Classification and regression trees*, Wadsworth international group, Belmont, California, USA, 1984.
- [115] T. Skwarnicki, *A study of the radiative cascade transitions between the Upsilon-prime and Upsilon resonances*, PhD thesis, Institute of Nuclear Physics, Krakow, 1986, DESY-F31-86-02.
- [116] See Supplemental Material at [URL will be inserted by publisher] for further details.
- [117] S. S. Wilks, *The large-sample distribution of the likelihood ratio for testing composite hypotheses*, Ann. Math. Stat. **9** (1938) 60.
- [118] D. M. Straub, *flavio: a Python package for flavour and precision phenomenology in the Standard Model and beyond*, [arXiv:1810.08132](https://arxiv.org/abs/1810.08132).

K.M. Fischer⁶³, D.S. Fitzgerald⁸⁷, C. Fitzpatrick⁶², T. Fiutowski³⁴, A. Fkiaras⁴⁸, F. Fleuret¹², M. Fontana¹³, F. Fontanelli^{24,i}, R. Forty⁴⁸, D. Foulds-Holt⁵⁵, V. Franco Lima⁶⁰, M. Franco Sevilla⁶⁶, M. Frank⁴⁸, E. Franzoso²¹, G. Frau¹⁷, C. Frei⁴⁸, D.A. Friday⁵⁹, J. Fu⁶, Q. Fuehring¹⁵, E. Gabriel³², G. Galati^{19,d}, A. Gallas Torreira⁴⁶, D. Galli^{20,e}, S. Gambetta^{58,48}, Y. Gan³, M. Gandelman², P. Gandini²⁵, Y. Gao⁵, M. Garau²⁷, L.M. Garcia Martin⁵⁶, P. Garcia Moreno⁴⁵, J. Garcia Pardiñas^{26,k}, B. Garcia Plana⁴⁶, F.A. Garcia Rosales¹², L. Garrido⁴⁵, C. Gaspar⁴⁸, R.E. Geertsema³², D. Gerick¹⁷, L.L. Gerken¹⁵, E. Gersabeck⁶², M. Gersabeck⁶², T. Gershon⁵⁶, D. Gerstel¹⁰, L. Giambastiani²⁸, V. Gibson⁵⁵, H.K. Giemza³⁶, A.L. Gilman⁶³, M. Giovannetti^{23,q}, A. Gioventù⁴⁶, P. Gironella Gironell⁴⁵, C. Giugliano^{21,g}, K. Gizdov⁵⁸, E.L. Gkougkousis⁴⁸, V.V. Gligorov¹³, C. Göbel⁷⁰, E. Golobardes⁸⁵, D. Golubkov⁴¹, A. Golutvin^{61,83}, A. Gomes^{1,a}, S. Gomez Fernandez⁴⁵, F. Goncalves Abrantes⁶³, M. Goncerz³⁵, G. Gong³, P. Gorbounov⁴¹, I.V. Gorelov⁴⁰, C. Gotti²⁶, E. Govorkova⁴⁸, J.P. Grabowski¹⁷, T. Grammatico¹³, L.A. Granado Cardoso⁴⁸, E. Graugés⁴⁵, E. Graverini⁴⁹, G. Graziani²², A. Grecu³⁷, L.M. Greeven³², N.A. Grieser⁴, L. Grillo⁶², S. Gromov⁸³, B.R. Gruberg Cazon⁶³, C. Gu³, M. Guarise²¹, M. Guittiere¹¹, P. A. Günther¹⁷, E. Gushchin³⁹, A. Guth¹⁴, Y. Guz⁴⁴, T. Gys⁴⁸, T. Hadavizadeh⁶⁹, G. Haefeli⁴⁹, C. Haen⁴⁸, J. Haimberger⁴⁸, T. Halewood-leagas⁶⁰, P.M. Hamilton⁶⁶, J.P. Hammerich⁶⁰, Q. Han⁷, X. Han¹⁷, T.H. Hancock⁶³, E.B. Hansen⁶², S. Hansmann-Menzemer¹⁷, N. Harnew⁶³, T. Harrison⁶⁰, C. Hasse⁴⁸, M. Hatch⁴⁸, J. He^{6,b}, M. Hecker⁶¹, K. Heijhoff³², K. Heinicke¹⁵, R.D.L. Henderson^{69,56}, A.M. Hennequin⁴⁸, K. Hennessy⁶⁰, L. Henry⁴⁸, J. Heuel¹⁴, A. Hicheur², D. Hill⁴⁹, M. Hilton⁶², S.E. Hollitt¹⁵, R. Hou⁷, Y. Hou⁸, J. Hu¹⁷, J. Hu⁷², W. Hu⁷, X. Hu³, W. Huang⁶, X. Huang⁷³, W. Hulsbergen³², R.J. Hunter⁵⁶, M. Hushchyn⁸², D. Hutchcroft⁶⁰, D. Hynds³², P. Ibis¹⁵, M. Idzik³⁴, D. Iljin³⁸, P. Ilten⁶⁵, A. Inglessi³⁸, A. Ishteev⁸³, K. Ivshin³⁸, R. Jacobsson⁴⁸, H. Jage¹⁴, S. Jakobsen⁴⁸, E. Jans³², B.K. Jashal⁴⁷, A. Jawahery⁶⁶, V. Jevtic¹⁵, X. Jiang⁴, M. John⁶³, D. Johnson⁶⁴, C.R. Jones⁵⁵, T.P. Jones⁵⁶, B. Jost⁴⁸, N. Jurik⁴⁸, S.H. Kalavan Kadavath³⁴, S. Kandybei⁵¹, Y. Kang³, M. Karacson⁴⁸, M. Karpov⁸², J.W. Kautz⁶⁵, F. Keizer⁴⁸, D.M. Keller⁶⁸, M. Kenzie⁵⁶, T. Ketel³³, B. Khanji¹⁵, A. Kharisova⁸⁴, S. Kholodenko⁴⁴, T. Kirn¹⁴, V.S. Kirsebom⁴⁹, O. Kitouni⁶⁴, S. Klaver³², N. Kleijne²⁹, K. Klimaszewski³⁶, M.R. Kmiec³⁶, S. Koliiev⁵², A. Kondybayeva⁸³, A. Konoplyannikov⁴¹, P. Kopciewicz³⁴, R. Kopecna¹⁷, P. Koppenburg³², M. Korolev⁴⁰, I. Kostiuk^{32,52}, O. Kot⁵², S. Kotriakhova^{21,38}, P. Kravchenko³⁸, L. Kravchuk³⁹, R.D. Krawczyk⁴⁸, M. Kreps⁵⁶, F. Kress⁶¹, S. Kretzschmar¹⁴, P. Krokovny^{43,v}, W. Krupa³⁴, W. Krzemien³⁶, J. Kubat¹⁷, M. Kucharczyk³⁵, V. Kudryavtsev^{43,v}, H.S. Kuindersma^{32,33}, G.J. Kunde⁶⁷, T. Kvaratskheliya⁴¹, D. Lacarrere⁴⁸, G. Lafferty⁶², A. Lai²⁷, A. Lampis²⁷, D. Lancierini⁵⁰, J.J. Lane⁶², R. Lane⁵⁴, G. Lanfranchi²³, C. Langenbruch¹⁴, J. Langer¹⁵, O. Lantwin⁸³, T. Latham⁵⁶, F. Lazzari^{29,r}, R. Le Gac¹⁰, S.H. Lee⁸⁷, R. Lefèvre⁹, A. Leflat⁴⁰, S. Legotin⁸³, O. Leroy¹⁰, T. Lesiak³⁵, B. Leverington¹⁷, H. Li⁷², P. Li¹⁷, S. Li⁷, Y. Li⁴, Y. Li⁴, Z. Li⁶⁸, X. Liang⁶⁸, T. Lin⁶¹, R. Lindner⁴⁸, V. Lisovskyi¹⁵, R. Litvinov²⁷, G. Liu⁷², H. Liu⁶, Q. Liu⁶, S. Liu⁴, A. Lobo Salvia⁴⁵, A. Loi²⁷, J. Lomba Castro⁴⁶, I. Longstaff⁵⁹, J.H. Lopes², S. Lopez Solino⁴⁶, G.H. Lovell⁵⁵, Y. Lu⁴, C. Lucarelli^{22,h}, D. Lucchesi^{28,m}, S. Luchuk³⁹, M. Lucio Martinez³², V. Lukashenko^{32,52}, Y. Luo³, A. Lupato⁶², E. Luppi^{21,g}, O. Lupton⁵⁶, A. Lusiani^{29,n}, X. Lyu⁶, L. Ma⁴, R. Ma⁶, S. Maccolini^{20,e}, F. Machefert¹¹, F. Maciuc³⁷, V. Macko⁴⁹, P. Mackowiak¹⁵, S. Maddrell-Mander⁵⁴, O. Madejczyk³⁴, L.R. Madhan Mohan⁵⁴, O. Maev³⁸, A. Maevskiy⁸², M.W. Majewski³⁴, J.J. Malczewski³⁵, S. Malde⁶³, B. Malecki⁴⁸, A. Malinin⁸¹, T. Maltsev^{43,v}, H. Malygina¹⁷, G. Manca^{27,f}, G. Mancinelli¹⁰, D. Manuzzi^{20,e}, D. Marangotto^{25,j}, J. Maratas^{9,t}, J.F. Marchand⁸, U. Marconi²⁰, S. Mariani^{22,h}, C. Marin Benito⁴⁸, M. Marinangeli⁴⁹, J. Marks¹⁷, A.M. Marshall⁵⁴, P.J. Marshall⁶⁰, G. Martelli⁷⁸, G. Martellotti³⁰, L. Martinazzoli^{48,k}, M. Martinelli^{26,k}, D. Martinez Santos⁴⁶, F. Martinez Vidal⁴⁷, A. Massafferri¹, M. Materok¹⁴, R. Matev⁴⁸, A. Mathad⁵⁰, V. Matiunin⁴¹, C. Matteuzzi²⁶, K.R. Mattioli⁸⁷, A. Mauri³², E. Maurice¹², J. Mauricio⁴⁵, M. Mazurek⁴⁸, M. McCann⁶¹, L. Mcconnell¹⁸, T.H. McGrath⁶²,

N.T. McHugh⁵⁹, A. McNab⁶², R. McNulty¹⁸, J.V. Mead⁶⁰, B. Meadows⁶⁵, G. Meier¹⁵, D. Melnychuk³⁶, S. Meloni^{26,k}, M. Merk^{32,80}, A. Merli^{25,j}, L. Meyer Garcia², M. Mikhasenko^{75,c}, D.A. Milanes⁷⁴, E. Millard⁵⁶, M. Milovanovic⁴⁸, M.-N. Minard⁸, A. Minotti^{26,k}, L. Minzoni^{21,g}, S.E. Mitchell⁵⁸, B. Mitreska⁶², D.S. Mitzel¹⁵, A. Mödden¹⁵, R.A. Mohammed⁶³, R.D. Moise⁶¹, S. Mokhnenko⁸², T. Mombächer⁴⁶, I.A. Monroy⁷⁴, S. Monteil⁹, M. Morandin²⁸, G. Morello²³, M.J. Morello^{29,n}, J. Moron³⁴, A.B. Morris⁷⁵, A.G. Morris⁵⁶, R. Mountain⁶⁸, H. Mu³, F. Muheim^{58,48}, M. Mulder⁷⁹, D. Müller⁴⁸, K. Müller⁵⁰, C.H. Murphy⁶³, D. Murray⁶², R. Murta⁶¹, P. Muzzetto²⁷, P. Naik⁵⁴, T. Nakada⁴⁹, R. Nandakumar⁵⁷, T. Nanut⁴⁸, I. Nasteva², M. Needham⁵⁸, N. Neri^{25,j}, S. Neubert⁷⁵, N. Neufeld⁴⁸, R. Newcombe⁶¹, E.M. Niel¹¹, S. Nieswand¹⁴, N. Nikitin⁴⁰, N.S. Nolte⁶⁴, C. Normand⁸, C. Nunez⁸⁷, A. Oblakowska-Mucha³⁴, V. Obraztsov⁴⁴, T. Oeser¹⁴, D.P. O'Hanlon⁵⁴, S. Okamura²¹, R. Oldeman^{27,f}, F. Oliva⁵⁸, M.E. Olivares⁶⁸, C.J.G. Onderwater⁷⁹, R.H. O'Neil⁵⁸, J.M. Otalora Goicochea², T. Ovsiannikova⁴¹, P. Owen⁵⁰, A. Oyanguren⁴⁷, K.O. Padeken⁷⁵, B. Pagare⁵⁶, P.R. Pais⁴⁸, T. Pajero⁶³, A. Palano¹⁹, M. Palutan²³, Y. Pan⁶², G. Panshin⁸⁴, A. Papanestis⁵⁷, M. Pappagallo^{19,d}, L.L. Pappalardo^{21,g}, C. Pappenheimer⁶⁵, W. Parker⁶⁶, C. Parkes⁶², B. Passalacqua²¹, G. Passaleva²², A. Pastore¹⁹, M. Patel⁶¹, C. Patrignani^{20,e}, C.J. Pawley⁸⁰, A. Pearce^{48,57}, A. Pellegrino³², M. Pepe Altarelli⁴⁸, S. Perazzini²⁰, D. Pereima⁴¹, A. Pereiro Castro⁴⁶, P. Perret⁹, M. Petric^{59,48}, K. Petridis⁵⁴, A. Petrolini^{24,i}, A. Petrov⁸¹, S. Petrucci⁵⁸, M. Petruzzo²⁵, T.T.H. Pham⁶⁸, A. Philippov⁴², R. Piandani⁶, L. Pica^{29,n}, M. Piccini⁷⁸, B. Pietrzyk⁸, G. Pietrzyk⁴⁹, M. Pili⁶³, D. Pinci³⁰, F. Pisani⁴⁸, M. Pizzichemi^{26,48,k}, Resmi P.K¹⁰, V. Placinta³⁷, J. Plews⁵³, M. Plo Casasus⁴⁶, F. Polci¹³, M. Poli Lener²³, M. Poliakova⁶⁸, A. Poluektov¹⁰, N. Polukhina^{83,u}, I. Polyakov⁶⁸, E. Polycarpo², S. Ponce⁴⁸, D. Popov^{6,48}, S. Popov⁴², S. Poslavskii⁴⁴, K. Prasanth³⁵, L. Promberger⁴⁸, C. Prouve⁴⁶, V. Pugatch⁵², V. Puill¹¹, G. Punzi^{29,o}, H. Qi³, W. Qian⁶, N. Qin³, R. Quagliani⁴⁹, N.V. Raab¹⁸, R.I. Rabadan Trejo⁶, B. Rachwal³⁴, J.H. Rademacker⁵⁴, M. Rama²⁹, M. Ramos Pernas⁵⁶, M.S. Rangel², F. Ratnikov^{42,82}, G. Raven³³, M. Reboud⁸, F. Redi⁴⁹, F. Reiss⁶², C. Remon Alepuz⁴⁷, Z. Ren³, V. Renaudin⁶³, R. Ribatti²⁹, A.M. Ricci²⁷, S. Ricciardi⁵⁷, K. Rinnert⁶⁰, P. Robbe¹¹, G. Robertson⁵⁸, A.B. Rodrigues⁴⁹, E. Rodrigues⁶⁰, J.A. Rodriguez Lopez⁷⁴, E.R.R. Rodriguez Rodriguez⁴⁶, A. Rollings⁶³, P. Roloff⁴⁸, V. Romanovskiy⁴⁴, M. Romero Lamas⁴⁶, A. Romero Vidal⁴⁶, J.D. Roth⁸⁷, M. Rotondo²³, M.S. Rudolph⁶⁸, T. Ruf⁴⁸, R.A. Ruiz Fernandez⁴⁶, J. Ruiz Vidal⁴⁷, A. Ryzhikov⁸², J. Ryzka³⁴, J.J. Saborido Silva⁴⁶, N. Sagidova³⁸, N. Sahoo⁵⁶, B. Saitta^{27,f}, M. Salomoni⁴⁸, C. Sanchez Gras³², R. Santacesaria³⁰, C. Santamarina Rios⁴⁶, M. Santimaria²³, E. Santovetti^{31,q}, D. Saranin⁸³, G. Sarpis¹⁴, M. Sarpis⁷⁵, A. Sarti³⁰, C. Satriano^{30,p}, A. Satta³¹, M. Saur¹⁵, D. Savrina^{41,40}, H. Sazak⁹, L.G. Scantlebury Smead⁶³, A. Scarabotto¹³, S. Schael¹⁴, S. Scherl⁶⁰, M. Schiller⁵⁹, H. Schindler⁴⁸, M. Schmelling¹⁶, B. Schmidt⁴⁸, S. Schmitt¹⁴, O. Schneider⁴⁹, A. Schopper⁴⁸, M. Schubiger³², S. Schulte⁴⁹, M.H. Schune¹¹, R. Schwemmer⁴⁸, B. Sciascia^{23,48}, S. Sellam⁴⁶, A. Semennikov⁴¹, M. Senghi Soares³³, A. Sergi^{24,i}, N. Serra⁵⁰, L. Sestini²⁸, A. Seuthe¹⁵, Y. Shang⁵, D.M. Shangase⁸⁷, M. Shapkin⁴⁴, I. Shchemberov⁸³, L. Shchutska⁴⁹, T. Shears⁶⁰, L. Shekhtman^{43,v}, Z. Shen⁵, S. Sheng⁴, V. Shevchenko⁸¹, E.B. Shields^{26,k}, Y. Shimizu¹¹, E. Shmanin⁸³, J.D. Shupperd⁶⁸, B.G. Siddi²¹, R. Silva Coutinho⁵⁰, G. Simi²⁸, S. Simone^{19,d}, N. Skidmore⁶², T. Skwarnicki⁶⁸, M.W. Slater⁵³, I. Slazyk^{21,g}, J.C. Smallwood⁶³, J.G. Smeaton⁵⁵, A. Smetkina⁴¹, E. Smith⁵⁰, M. Smith⁶¹, A. Snoch³², L. Soares Lavra⁹, M.D. Sokoloff⁶⁵, F.J.P. Soler⁵⁹, A. Solovev³⁸, I. Solovyev³⁸, F.L. Souza De Almeida², B. Souza De Paula², B. Spaan¹⁵, E. Spadaro Norella^{25,j}, P. Spradlin⁵⁹, F. Stagni⁴⁸, M. Stahl⁶⁵, S. Stahl⁴⁸, S. Stanislaus⁶³, O. Steinkamp^{50,83}, O. Stenyakin⁴⁴, H. Stevens¹⁵, S. Stone^{68,48,†}, D. Strekalina⁸³, F. Suljik⁶³, J. Sun²⁷, L. Sun⁷³, Y. Sun⁶⁶, P. Svihra⁶², P.N. Swallow⁵³, K. Swientek³⁴, A. Szabelski³⁶, T. Szumlak³⁴, M. Szymanski⁴⁸, S. Taneja⁶², A.R. Tanner⁵⁴, M.D. Tat⁶³, A. Terentev⁸³, F. Teubert⁴⁸, E. Thomas⁴⁸, D.J.D. Thompson⁵³, K.A. Thomson⁶⁰, H. Tilquin⁶¹, V. Tisserand⁹, S. T'Jampens⁸, M. Tobin⁴, L. Tomassetti^{21,g}, X. Tong⁵,

D. Torres Machado¹, D.Y. Tou¹³, E. Trifonova⁸³, S.M. Trilov⁵⁴, C. Tripli⁴⁹, G. Tuci⁶, A. Tully⁴⁹, N. Tuning^{32,48}, A. Ukleja^{36,48}, D.J. Unverzagt¹⁷, E. Ursov⁸³, A. Usachov³², A. Ustyuzhanin^{42,82}, U. Uwer¹⁷, A. Vagner⁸⁴, V. Vagnoni²⁰, A. Valassi⁴⁸, G. Valenti²⁰, N. Valls Canudas⁸⁵, M. van Beuzekom³², M. Van Dijk⁴⁹, H. Van Hecke⁶⁷, E. van Herwijnen⁸³, M. van Veghel⁷⁹, R. Vazquez Gomez⁴⁵, P. Vazquez Regueiro⁴⁶, C. Vázquez Sierra⁴⁸, S. Vecchi²¹, J.J. Velthuis⁵⁴, M. Veltri^{22,s}, A. Venkateswaran⁶⁸, M. Veronesi³², M. Vesterinen⁵⁶, D. Vieira⁶⁵, M. Vieites Diaz⁴⁹, H. Viemann⁷⁶, X. Vilasis-Cardona⁸⁵, E. Vilella Figueras⁶⁰, A. Villa²⁰, P. Vincent¹³, F.C. Volle¹¹, D. Vom Bruch¹⁰, A. Vorobyev³⁸, V. Vorobyev^{43,v}, N. Voropaev³⁸, K. Vos⁸⁰, R. Waldi¹⁷, J. Walsh²⁹, C. Wang¹⁷, J. Wang⁵, J. Wang⁴, J. Wang³, J. Wang⁷³, M. Wang³, R. Wang⁵⁴, Y. Wang⁷, Z. Wang⁵⁰, Z. Wang³, Z. Wang⁶, J.A. Ward^{56,69}, N.K. Watson⁵³, S.G. Weber¹³, D. Websdale⁶¹, C. Weisser⁶⁴, B.D.C. Westhenry⁵⁴, D.J. White⁶², M. Whitehead⁵⁴, A.R. Wiederhold⁵⁶, D. Wiedner¹⁵, G. Wilkinson⁶³, M. Wilkinson⁶⁸, I. Williams⁵⁵, M. Williams⁶⁴, M.R.J. Williams⁵⁸, F.F. Wilson⁵⁷, W. Wislicki³⁶, M. Witek³⁵, L. Witola¹⁷, G. Wormser¹¹, S.A. Wotton⁵⁵, H. Wu⁶⁸, K. Wyllie⁴⁸, Z. Xiang⁶, D. Xiao⁷, Y. Xie⁷, A. Xu⁵, J. Xu⁶, L. Xu³, M. Xu⁷, Q. Xu⁶, Z. Xu⁹, Z. Xu⁶, D. Yang³, S. Yang⁶, Y. Yang⁶, Z. Yang⁵, Z. Yang⁶⁶, Y. Yao⁶⁸, L.E. Yeomans⁶⁰, H. Yin⁷, J. Yu⁷¹, X. Yuan⁶⁸, O. Yushchenko⁴⁴, E. Zaffaroni⁴⁹, M. Zavertyaev^{16,u}, M. Zdybal³⁵, O. Zenaiev⁴⁸, M. Zeng³, D. Zhang⁷, L. Zhang³, S. Zhang⁷¹, S. Zhang⁵, Y. Zhang⁵, Y. Zhang⁶³, A. Zharkova⁸³, A. Zhelezov¹⁷, Y. Zheng⁶, T. Zhou⁵, X. Zhou⁶, Y. Zhou⁶, V. Zhovkovska¹¹, X. Zhu³, X. Zhu⁷, Z. Zhu⁶, V. Zhukov^{14,40}, J.B. Zonneveld⁵⁸, Q. Zou⁴, S. Zucchelli^{20,e}, D. Zuliani²⁸, G. Zunică⁶².

¹Centro Brasileiro de Pesquisas Físicas (CBPF), Rio de Janeiro, Brazil

²Universidade Federal do Rio de Janeiro (UFRJ), Rio de Janeiro, Brazil

³Center for High Energy Physics, Tsinghua University, Beijing, China

⁴Institute Of High Energy Physics (IHEP), Beijing, China

⁵School of Physics State Key Laboratory of Nuclear Physics and Technology, Peking University, Beijing, China

⁶University of Chinese Academy of Sciences, Beijing, China

⁷Institute of Particle Physics, Central China Normal University, Wuhan, Hubei, China

⁸Univ. Savoie Mont Blanc, CNRS, IN2P3-LAPP, Annecy, France

⁹Université Clermont Auvergne, CNRS/IN2P3, LPC, Clermont-Ferrand, France

¹⁰Aix Marseille Univ, CNRS/IN2P3, CPPM, Marseille, France

¹¹Université Paris-Saclay, CNRS/IN2P3, IJCLab, Orsay, France

¹²Laboratoire Leprince-Ringuet, CNRS/IN2P3, Ecole Polytechnique, Institut Polytechnique de Paris, Palaiseau, France

¹³LPNHE, Sorbonne Université, Paris Diderot Sorbonne Paris Cité, CNRS/IN2P3, Paris, France

¹⁴I. Physikalisches Institut, RWTH Aachen University, Aachen, Germany

¹⁵Fakultät Physik, Technische Universität Dortmund, Dortmund, Germany

¹⁶Max-Planck-Institut für Kernphysik (MPIK), Heidelberg, Germany

¹⁷Physikalisches Institut, Ruprecht-Karls-Universität Heidelberg, Heidelberg, Germany

¹⁸School of Physics, University College Dublin, Dublin, Ireland

¹⁹INFN Sezione di Bari, Bari, Italy

²⁰INFN Sezione di Bologna, Bologna, Italy

²¹INFN Sezione di Ferrara, Ferrara, Italy

²²INFN Sezione di Firenze, Firenze, Italy

²³INFN Laboratori Nazionali di Frascati, Frascati, Italy

²⁴INFN Sezione di Genova, Genova, Italy

²⁵INFN Sezione di Milano, Milano, Italy

²⁶INFN Sezione di Milano-Bicocca, Milano, Italy

²⁷INFN Sezione di Cagliari, Monserrato, Italy

²⁸Universita degli Studi di Padova, Universita e INFN, Padova, Padova, Italy

²⁹INFN Sezione di Pisa, Pisa, Italy

³⁰INFN Sezione di Roma La Sapienza, Roma, Italy

³¹INFN Sezione di Roma Tor Vergata, Roma, Italy

- ³²*Nikhef National Institute for Subatomic Physics, Amsterdam, Netherlands*
- ³³*Nikhef National Institute for Subatomic Physics and VU University Amsterdam, Amsterdam, Netherlands*
- ³⁴*AGH - University of Science and Technology, Faculty of Physics and Applied Computer Science, Kraków, Poland*
- ³⁵*Henryk Niewodniczanski Institute of Nuclear Physics Polish Academy of Sciences, Kraków, Poland*
- ³⁶*National Center for Nuclear Research (NCBJ), Warsaw, Poland*
- ³⁷*Horia Hulubei National Institute of Physics and Nuclear Engineering, Bucharest-Magurele, Romania*
- ³⁸*Petersburg Nuclear Physics Institute NRC Kurchatov Institute (PNPI NRC KI), Gatchina, Russia*
- ³⁹*Institute for Nuclear Research of the Russian Academy of Sciences (INR RAS), Moscow, Russia*
- ⁴⁰*Institute of Nuclear Physics, Moscow State University (SINP MSU), Moscow, Russia*
- ⁴¹*Institute of Theoretical and Experimental Physics NRC Kurchatov Institute (ITEP NRC KI), Moscow, Russia*
- ⁴²*Yandex School of Data Analysis, Moscow, Russia*
- ⁴³*Budker Institute of Nuclear Physics (SB RAS), Novosibirsk, Russia*
- ⁴⁴*Institute for High Energy Physics NRC Kurchatov Institute (IHEP NRC KI), Protvino, Russia, Protvino, Russia*
- ⁴⁵*ICCUB, Universitat de Barcelona, Barcelona, Spain*
- ⁴⁶*Instituto Galego de Física de Altas Enerxías (IGFAE), Universidade de Santiago de Compostela, Santiago de Compostela, Spain*
- ⁴⁷*Instituto de Fisica Corpuscular, Centro Mixto Universidad de Valencia - CSIC, Valencia, Spain*
- ⁴⁸*European Organization for Nuclear Research (CERN), Geneva, Switzerland*
- ⁴⁹*Institute of Physics, Ecole Polytechnique Fédérale de Lausanne (EPFL), Lausanne, Switzerland*
- ⁵⁰*Physik-Institut, Universität Zürich, Zürich, Switzerland*
- ⁵¹*NSC Kharkiv Institute of Physics and Technology (NSC KIPT), Kharkiv, Ukraine*
- ⁵²*Institute for Nuclear Research of the National Academy of Sciences (KINR), Kyiv, Ukraine*
- ⁵³*University of Birmingham, Birmingham, United Kingdom*
- ⁵⁴*H.H. Wills Physics Laboratory, University of Bristol, Bristol, United Kingdom*
- ⁵⁵*Cavendish Laboratory, University of Cambridge, Cambridge, United Kingdom*
- ⁵⁶*Department of Physics, University of Warwick, Coventry, United Kingdom*
- ⁵⁷*STFC Rutherford Appleton Laboratory, Didcot, United Kingdom*
- ⁵⁸*School of Physics and Astronomy, University of Edinburgh, Edinburgh, United Kingdom*
- ⁵⁹*School of Physics and Astronomy, University of Glasgow, Glasgow, United Kingdom*
- ⁶⁰*Oliver Lodge Laboratory, University of Liverpool, Liverpool, United Kingdom*
- ⁶¹*Imperial College London, London, United Kingdom*
- ⁶²*Department of Physics and Astronomy, University of Manchester, Manchester, United Kingdom*
- ⁶³*Department of Physics, University of Oxford, Oxford, United Kingdom*
- ⁶⁴*Massachusetts Institute of Technology, Cambridge, MA, United States*
- ⁶⁵*University of Cincinnati, Cincinnati, OH, United States*
- ⁶⁶*University of Maryland, College Park, MD, United States*
- ⁶⁷*Los Alamos National Laboratory (LANL), Los Alamos, United States*
- ⁶⁸*Syracuse University, Syracuse, NY, United States*
- ⁶⁹*School of Physics and Astronomy, Monash University, Melbourne, Australia, associated to ⁵⁶*
- ⁷⁰*Pontifícia Universidade Católica do Rio de Janeiro (PUC-Rio), Rio de Janeiro, Brazil, associated to ²*
- ⁷¹*Physics and Micro Electronic College, Hunan University, Changsha City, China, associated to ⁷*
- ⁷²*Guangdong Provincial Key Laboratory of Nuclear Science, Guangdong-Hong Kong Joint Laboratory of Quantum Matter, Institute of Quantum Matter, South China Normal University, Guangzhou, China, associated to ³*
- ⁷³*School of Physics and Technology, Wuhan University, Wuhan, China, associated to ³*
- ⁷⁴*Departamento de Fisica , Universidad Nacional de Colombia, Bogota, Colombia, associated to ¹³*
- ⁷⁵*Universität Bonn - Helmholtz-Institut für Strahlen und Kernphysik, Bonn, Germany, associated to ¹⁷*
- ⁷⁶*Institut für Physik, Universität Rostock, Rostock, Germany, associated to ¹⁷*
- ⁷⁷*Eotvos Lorand University, Budapest, Hungary, associated to ⁴⁸*
- ⁷⁸*INFN Sezione di Perugia, Perugia, Italy, associated to ²¹*
- ⁷⁹*Van Swinderen Institute, University of Groningen, Groningen, Netherlands, associated to ³²*
- ⁸⁰*Universiteit Maastricht, Maastricht, Netherlands, associated to ³²*

⁸¹*National Research Centre Kurchatov Institute, Moscow, Russia, associated to* ⁴¹

⁸²*National Research University Higher School of Economics, Moscow, Russia, associated to* ⁴²

⁸³*National University of Science and Technology “MISIS”, Moscow, Russia, associated to* ⁴¹

⁸⁴*National Research Tomsk Polytechnic University, Tomsk, Russia, associated to* ⁴¹

⁸⁵*DS4DS, La Salle, Universitat Ramon Llull, Barcelona, Spain, associated to* ⁴⁵

⁸⁶*Department of Physics and Astronomy, Uppsala University, Uppsala, Sweden, associated to* ⁵⁹

⁸⁷*University of Michigan, Ann Arbor, United States, associated to* ⁶⁸

^a*Universidade Federal do Triângulo Mineiro (UFTM), Uberaba-MG, Brazil*

^b*Hangzhou Institute for Advanced Study, UCAS, Hangzhou, China*

^c*Excellence Cluster ORIGINS, Munich, Germany*

^d*Università di Bari, Bari, Italy*

^e*Università di Bologna, Bologna, Italy*

^f*Università di Cagliari, Cagliari, Italy*

^g*Università di Ferrara, Ferrara, Italy*

^h*Università di Firenze, Firenze, Italy*

ⁱ*Università di Genova, Genova, Italy*

^j*Università degli Studi di Milano, Milano, Italy*

^k*Università di Milano Bicocca, Milano, Italy*

^l*Università di Modena e Reggio Emilia, Modena, Italy*

^m*Università di Padova, Padova, Italy*

ⁿ*Scuola Normale Superiore, Pisa, Italy*

^o*Università di Pisa, Pisa, Italy*

^p*Università della Basilicata, Potenza, Italy*

^q*Università di Roma Tor Vergata, Roma, Italy*

^r*Università di Siena, Siena, Italy*

^s*Università di Urbino, Urbino, Italy*

^t*MSU - Iligan Institute of Technology (MSU-IIT), Iligan, Philippines*

^u*P.N. Lebedev Physical Institute, Russian Academy of Science (LPI RAS), Moscow, Russia*

^v*Novosibirsk State University, Novosibirsk, Russia*

[†]*Deceased*